Joachim Höpfner

Seasonal variations in length of day and atmospheric angular momentum

Paper presented
at the XXII General Assembly
European Geophysical Society
Vienna, Austria, 21-25 April 1997

Scientific Technical Report STR97/08

Publication: Scientific Technical Report
No.: STR97/08

Seasonal variations in length of day and atmospheric angular momentum

Joachim Höpfner

GeoForschungsZentrum Potsdam, Division 1: Kinematics and Dynamics of the Earth,Telegrafenberg, D-14473 Potsdam, Germany; E-mail: ho@gfz-potsdam.de

Abstract. Seasonal Earth's rotation variations are still not sufficiently explained concerning their causes. It should be noted that quantitative estimates of the variability of the oscillations in Length-Of-Day (LOD) and Atmospheric-Angular-Momentum (AAM) were applied very seldom. Therefore, the problem is re-examined.

Especially, the axial AAM component labelled χ_3 is related to changes in LOD. For that reason, the following series of data at one-day intervals are used in this study: (a) LOD of the series EOP(IERS)C04 from 1962 to 1996, (b) χ_3(W), χ_3(P) and χ_3(P+IB) of the series AAM(NMC) from 1976 to 1995 and (c) χ_3(W), χ_3(P) and χ_3(P+IB) of the series AAM(JMA) from 1983 to 1995. Here, χ_3(W) is the wind term, χ_3(P) the pressure term and χ_3(P+IB) the pressure term with inverted barometer response.

First, the seasonal oscillations are separated by filtering from the different time series. To illustrate their characteristics, the amplitudes, periods and phases of the annual and semiannual oscillations are then derived in their temporal variability. The discrepancies between the quantities of the annual and semiannual components of LOD without the tidal effects Sa as well as Ssa and χ_3(W), χ_3(W)+χ_3(P) as well as χ_3(W)+χ_3(P+IB) show to which extent uncertainties are present in the data, which portions of AAM originate from χ_3(W), χ_3(P) and χ_3(P+IB), respectively, and whether another excitation source contributes to seasonal LOD variations. At the annual frequency, the wind term neglected still from the upper stratosphere is evidently responsible for the imbalance between the LOD and AAM data. However, at the semiannual frequency, the discrepancy is not fully explained by the missing stratospheric wind term, and a contribution from the global surface water redistribution is likely.

Key words: Earth's rotation, LOD (length of day), AAM (atmospheric angular momentum), seasonal oscillations, axial angular momentum budget, imbalance

1 Introduction

Earth rotation and polar motion variations are mainly caused by dynamic processes due to mass redistributions under the conservation of the total angular momentum of entire Earth. In these processes, the dominant forcing is of atmospheric origin. Variations in Atmospheric-Angular-Momentum (AAM) are mirrored clearly in Earth's rotation signals on many time scales. The hydrosphere is another excitation source.

Seasonal changes in Length-Of-Day (LOD) represent the largest signal in this quantity on less than decadal periods and are, therefore, of fundamental importance. They are mainly attributed to the exchange of axial angular momentum between the atmosphere and the solid Earth. It should be noted that the main contributions to the axial AAM component are global zonal winds in the troposphere and the stratosphere. There are still small significant discrepancies in the solid Earth-atmosphere momentum budget derived from high-quality data sets at seasonal frequencies. The subject of this paper is to study the amplitude, phase and period of the seasonal oscillations in LOD and AAM in their temporal variability and to quantify better the discrepancies between the LOD and AAM estimates in search of their sources.

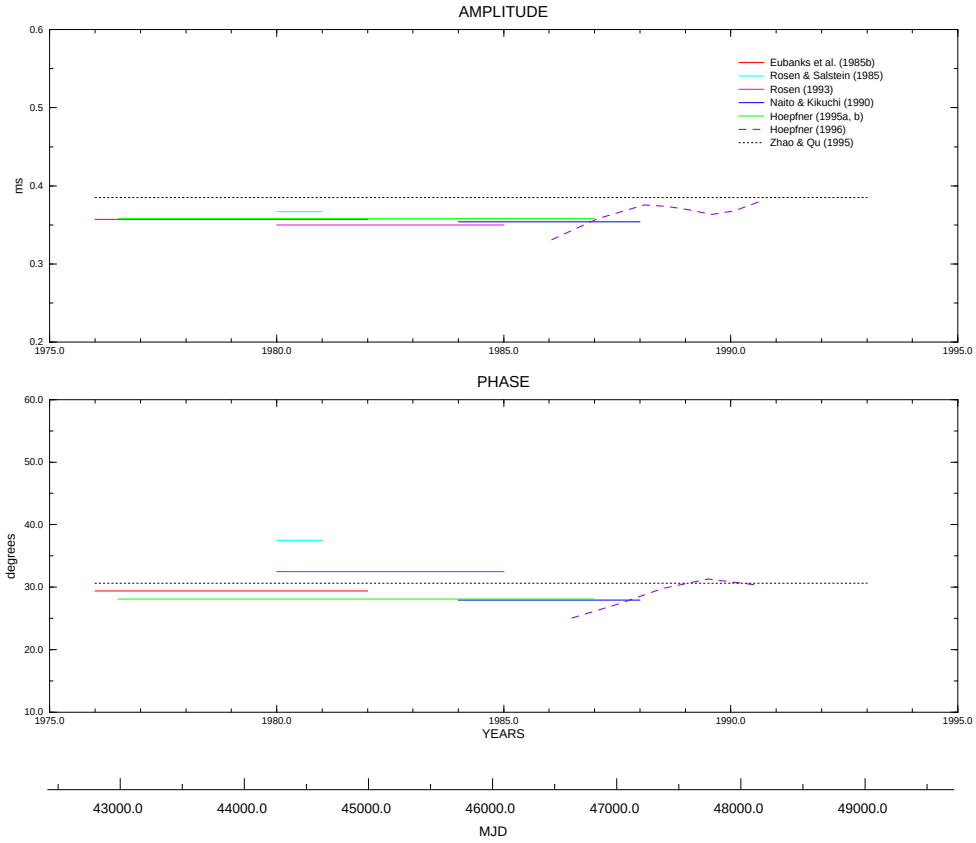

Figure 1. Amplitude (top) and phase (bottom) estimates of the annual oscillation in Length-Of-Day from different data

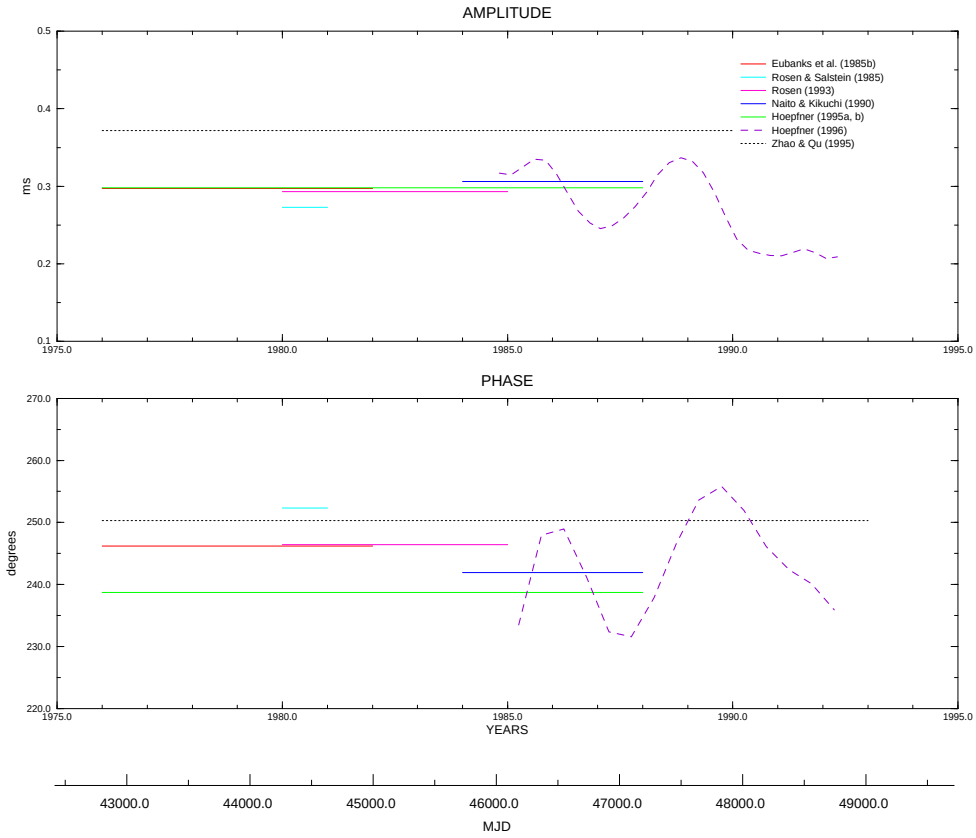

Figure 2. Same as Fig. 1, but for the semiannual oscillation in Length-Of-Day

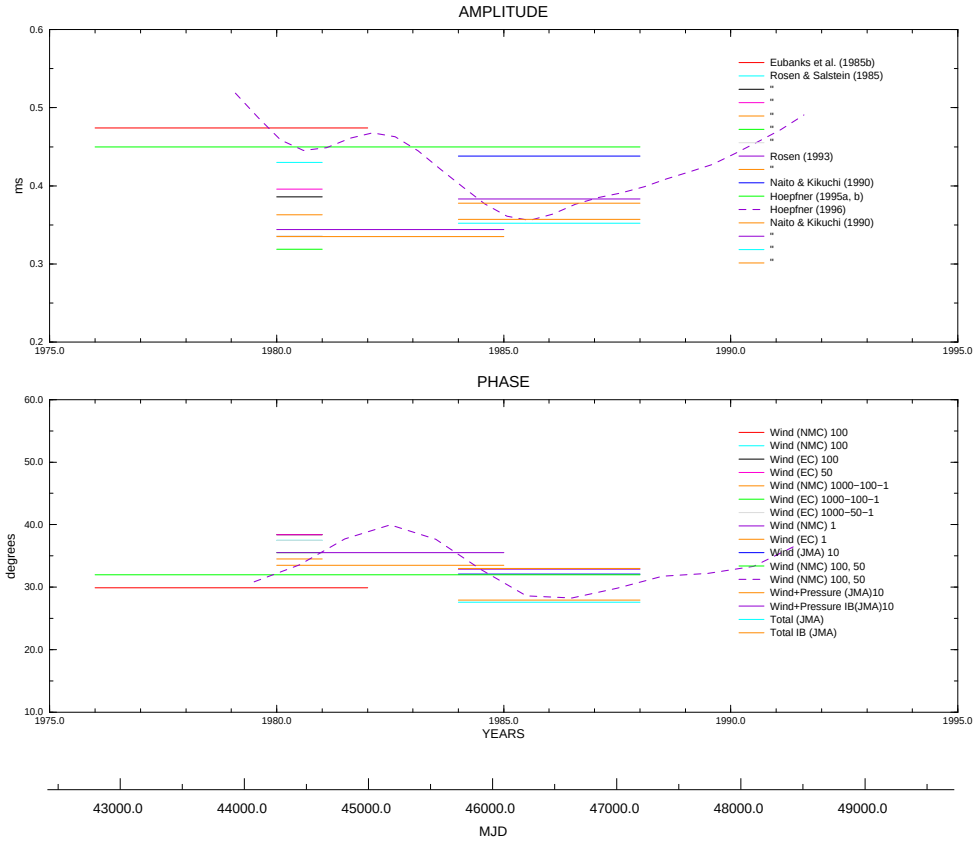

Figure 3. Amplitude (top) and phase (bottom) estimates of the contributions to annual oscillation in Length-Of-Day from different data

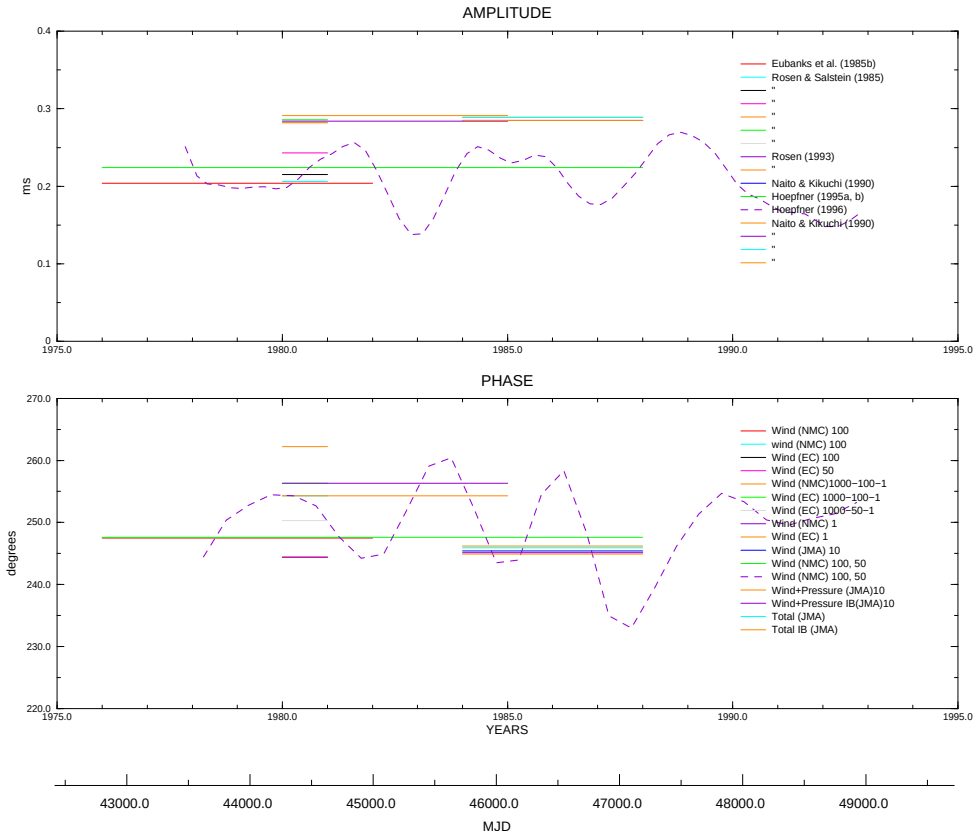

Figure 4. Same as Fig. 3, but for the semiannual oscillation in Length-Of-Day

Table 1. Seasonal oscillations in LOD from different data. The phase angle refers to January 1 with respect to the cosine convention

Term	Period	Annual oscillation		Semiannual oscillation		Source
		Amplitude (in ms)	Phase (in degrees)	Amplitude (in ms)	Phase (in degrees)	
LOD (BIH)	1976 ... 1982	0.357	29.4	0.297	246.2	Eubanks et al. (1985)
LOD (LLR)		0.357	29.5	0.315	248.4	
LOD (VLBI, SLR, LLR)	1980 ... 1981	0.367	37.5	0.273	252.3	Rosen & Salstein (1985)
LOD (VLBI, SLR, LLR)	1980 ... 1985	0.350	32.5	0.293	246.4	Rosen (1993)
LOD (IRIS)	1984 ... 1988	0.354	27.9	0.306	241.9	Naito & Kikuchi (1990)
LOD (IERS)	1976 ... 1988	0.358	28.1	0.298	238.7	Höpfner (1995a, b)
LOD (SLR)	1983 ... 1993	0.333 ... 0.386	25.5 ... 35.2	0.207 ... 0.346	231.6 ... 258.3	Höpfner (1996)
LOD (Analytical solution)		0.385	30.6	0.372	250.3	Zhao & Qu (1995)

2 State of the art in studying the Earth's axial angular momentum balance at seasonal periods

It is appropriate to briefly review some previous studies on the seasonal changes in LOD and AAM. There are the efforts pertaining to geodetic-astronomical time determinations and keeping the time using pendulum clocks since about 1890. The international activities in the field of the study of the Earth's rotation go back to 1898, when the International Latitude Service began to monitor the motion of the Earth's pole of rotation by star observations at six stations. The classical method for measuring polar motion and LOD is based on observing transit times of stars at a network of observatories worldwide. Seasonal variations in the Earth's rotation were first detected using quartz clocks in the mid-thirties (Pavel and Uhink 1935; Stoyko 1936). Until the introduction of the atomic time scale in July 1955, the investigations of this problem were difficult because of clock instabilities. Several new space-based techniques have recently been introduced for Earth rotation measurement. These include Very Long Baseline Interferometry (VLBI), Satellite Laser Ranging (SLR), and Lunar Laser Ranging (LLR). The data from each of these techniques span somewhat different periods and involve different temporal resolutions. Most recently, the Global Positioning System (GPS) has become available to measure the Earth Orientation Parameters (EOP).

Munk and Miller (1950) showed that seasonal changes in LOD could be explained by changes in AAM. Munk and MacDonald (1960) then concluded that the seasonal Earth's rotation variations are mainly driven by the exchange of axial angular momentum between the atmosphere and the solid Earth on this time scale. For the first time, Hide et al. (1980) computed the AAM using zonal wind fields produced daily for the entire Earth by two operational national weather services, the U. S. National Meteorological Center (NMC) and the United Kingdom Meteorological Office (UKMO), for their weather forecasting efforts and examined the short-term variations in the solid Earth-atmosphere momentum budget for a 4-month period considerably. Barnes et al. (1983) proposed effective AAM functions by which atmospheric motions and mass distribution can be related to Earth rotation and polar motion. Beginning January 1, 1976, a series of high-quality, daily AAM values computed as the atmosphere's three-dimensional angular momentum vector has become available from NMC. A second series of estimates of various AAM components is produced by the Japan Meteorological Agency (JMA) starting on September 28, 1983. The United Kingdom Meteorological Office (UKMO) also provides the data sets since that date. In addition, the European Centre for Medium Range Weather Forecasts (ECMWF or EC) produces operationally the AAM estimates since 1986.

The independent improvements in geodetic and atmospheric measurements of the relevant geophysical parameters have enabled remarkable advances in the study of Earth's variable rate of rotation and the role of the atmosphere in contributing to this variability for the close relationship between changes in the axial component of the angular momentum of the atmosphere and that of the solid Earth. For an overview of recent advances in the understanding of Earth's axial momentum balance on intraseasonal through interannual and decadal time scales see Hide and Dickey (1991) and also Rosen (1993). As mentioned above, the review here is restricted to the progress at seasonal periods.

Prior to the eighties, studies relating LOD and AAM dealt mostly with seasonal time scales because of data constraints. The results involved large uncertainties because of the limited quality of the input data sets. It was repeatedly found that the seasonal changes in LOD are caused by seasonal changes in AAM. In addition, there was a considerable discrepancy in the seasonal angular momentum budget of the global solid Earth-atmosphere system. The ensuing decades saw a number of studies aimed at better quantifying the relationship between AAM and LOD. Eubanks, Steppe and Dickey (1985a) found significant discrepancies between the angular momentum time series computed for the Earth and the atmosphere with high-resolution data sets at seasonal periods. But winds at pressures of less than 100 hPa, changes in the atmospheric pressure, and the response of the oceans to changes in the atmosphere pressure, among other effects, were all ignored in the study. By having their upper boundaries limited to either 100 or 50 hPa, the NMC AAM data sets do not

Table 2. Contributions to seasonal oscillations in LOD from different data. The phase angle refers to January 1 with respect to the cosine convention

Term	Period	Annual oscillation		Semiannual oscillation		Source
		Amplitude (in ms)	Phase (in degrees)	Amplitude (ms)	Phase (in degrees)	
Wind (NMC) (100)	1976 ... 1982	0.474	29.9	0.204	247.5	Eubanks et al. (1985b)
Wind (NMC) (100)	1980 ... 1981	0.430	37.5	0.206	254.3	Rosen & Salstein (1985)
(EC) (100)		0.386	38.4	0.215	244.4	
(EC) (50)		0.396	38.4	0.243	244.4	
(NMC) (1000-100-1)		0.363	34.5	0.282	262.2	
(EC) (1000-100-1)		0.319	35.5	0.286	256.3	
(EC) (1000-50-1)		0.336	37.5	0.281	250.3	
Wind (NMC) (1)	1980 ... 1985	0.344	35.5	0.284	256.3	Rosen (1993)
Wind (EC) (1)		0.335	33.5	0.291	254.3	
Wind (JMA) (10)	1984 ... 1988	0.438	32.1	0.285	245.4	Naito & Kikuchi (1990)
Wind (NMC) (100, 50)	1976 ... 1988	0.450	32.0	0.224	247.6	Höpfner (1995a, b)
Wind (NMC) (100, 50)	1976 ... 1993	0.353 ... 0.504	23.8 ... 41.9	0.138 ... 0.268	230.9 ... 260.1	Höpfner (1996)
Pressure (JMA)	1984 ... 1988	0.067	236.3	0.005	209.2	Naito & Kikuchi (1990)
Pressure with IB (JMA)		0.056	206.8	0.002	172.4	
Surface water storage		0.024	206.0	0.009	358.0	Chao & O'Connor(1988)
Antarctic Circum-Polar Current	1977 ... 1982	0.003	311.4	0.005	200.1	Whitworth & Peterson (1985)

incorporate much of the stratosphere. Therefore, most previous studies of the Earth-atmosphere momentum budget were not able to achieve a balanced budget at these time scales. Rosen and Salstein (1985) showed that the momentum in this portion of the atmosphere can account for the discrepancies previously found in the annual and semiannual components of the solid Earth-atmosphere momentum budget. Another process capable of exciting changes in LOD not considered involves the meridional shifting of air mass. Naito and Kikuchi (1990) demonstrated that redistribution of air mass and surface water storage contribute to reducing the seasonal imbalances in the solid Earth-atmosphere momentum budget. For the annual period, Gu and Paquet (1993) concluded that the shortfall is likely originated by the solar wind. Höpfner (1996) presented quantitative estimates of the seasonal oscillations in LOD and AAM in their temporal variability and the consequent imbalances in the seasonal momentum budgets of the global Earth-atmosphere system.

Some of the previous estimates of the annual and semiannual oscillations derived for LOD are summarized in Table 1. Also, an analytical solution obtained by Zhao and Qu (1995) is listed. The results are illustrated in Fig. 1 for the annual component and in Fig. 2 for the semiannual component. For comparison of the LOD estimates with those of the excitation contributions, the latter are given in Table 2. Besides the AAM estimates, the contribution from surface water storage estimated by Chao and O'Connor (1988) and that from the Antarctic Circum-Polar Current based upon volume transport data by Whitworth and Peterson (1985) and evaluated by Naito and Kikuchi (1990) are presented. Analogous to Figs 1 and 2, these estimates are plotted in Figs 3 and 4, respectively. The expressions for the seasonal components have the form $c\ \cos(2\pi t/T - \alpha)$, where c is the amplitude, α the phase, and T the annual and semiannual periods, respectively.

Concerning the wind terms, it should be noted that the added numbers are to reflect the upper level in the atmosphere in hPa used in calculating the AAM values. For instance, a series of Wind (NMC) (50) values incorporates zonal wind fields at levels from 1000 hPa up to and including 50 hPa (approximately 21 km altitude) provided by the NMC. Moreover, pressure terms are the AAM due to the global pressure field assuming either non-IB or IB conditions, where IB stands for the inverted-barometer effect, i. e. isostatic response of oceans to pressure variations.

Some limitations of the previous studies should be pointed out: Firstly, there are the limited sizes of the samples originating from different data sources. Secondly, the estimates represent average values over the study periods, except those by Gu and Paquet (1993) as well as Höpfner (1996). As the results listed here clearly show, there exist notable discrepancies among the amplitude and phase estimates. Indeed, some discrepancies may be due to limitations in the time series used. Other discrepancies, especially those between LOD and AAM estimates, however, are likely to reflect the presence of nonatmospheric contributions to the global momentum budget. It is very likely that the additional source is the hydrological budget. But, compared to the atmospheric contribution the hydrological one is less well determined because of lack of pertinent observations and the difficulty in its modelling in a realistic manner. Quantities that are difficult to measure are the redistributions of ground water, variations in global sea level, and changes in the strength of ocean currents such as the Antarctic Circum-Polar Current. Because modern and accurate geodetic and atmospheric data sets now span a period longer than a decade, they can be used to re-examine the character of the seasonal variations in LOD and AAM with time and to document the discrepancies that currently exist in the solid Earth-atmosphere momentum

Table 3. Characteristics of the LOD data of the series EOP(IERS)C04 (from eopc04.guide)

Period	Characteristics of the smoothing (in days)	Uncertainty of one daily value (in 0.1 ms)	Consistency with reference frames (in 0.1 ms)
1962 ... 1967	17	14	0
1968 ... 1971	17	10	0
1972 ... 1979	15	7	0
1980 ... 1983	10	3	0
1984 ... 1987	3	0.3	0
1988 ... present	3	0.3	0

budget at the seasonal frequencies. For further studies of the subject, the seasonal behavior in the residual series formed by subtracting the AAM from the LOD values is of importance. It should contribute to clarifying the role of the hydrological budget.

3 Data sets used in this study

3.1 LOD series

The Earth Orientation Parameters (EOP) are the quantities that describe the rotation of the International Terrestrial Reference System to the International Celestial Reference System, in conjunction with the conventional precession-nutation model. The International Earth Rotation Service (IERS) was created in 1988 by the International Union of Geodesy and Geophysics (IUGG) and the International Astronomical Union (IAU). Among other tasks, it is responsible for determining the values of EOP. For this purpose, it produces four combined EOP time series from the individual series received from the operational analysis centres. The series entering into the combination are selected on the basis of consistency with the reference frames and IERS Standards as well as duration, measurement frequency and precision (see, e. g. IERS 1995).

The series EOP(IERS)C04 is a continuous series at one-day intervals since 1962. It was computed over six intervals, 1962-1967, 1968-1971, 1972-1979, 1980-1983, 1984-1987 and 1988-present. It is homogenized, merged and then slightly smoothed. The data set used in this study is the following time series: LOD of the series EOP(IERS)C04 from January 1, 1962 to June 11, 1996, i. e. Modified Julian Date (MJD) from 37665.0 to 50245.0, where LOD is the excess of the duration of the day relative to 86400 s. The oscillations in the duration of the days due to zonal tides for periods below 35 days are present in a full magnitude in the series. The characteristics of the LOD data are given in Table 3. Note how the uncertainty improves by replacing the classical method for measuring such changes by space-based techniques over the periods.

A plot of the LOD series for the entire 34.5-year period from 1962 to 1996 is shown in Fig. 5. Also displayed is the trend of LOD obtained by low-pass filtering of the original data. For a discussion of the separation of the major components, namely trend and seasonal oscillations, see Section 5.

Table 4. Characteristics of the AAM data as computed by the NMC and JMA.There are only daily χ_1(W), χ_2(W) and χ_3(W) values based on the NMC data during 44605.5 to 45577.5

Weather center	Entire time span	Period (in MJD)	Sampling interval (in days)	Source data	Top level	Surface pressure
NMC	July 1976 ... Dec. 1995	42960.0 ... 44605.0	1.0	Initialized-phase data	100 hPa; 50 hPa	On model mountains
		44605.5 ... 48793.5	0.5		since Jan. 1981	
		48794.25 ... 50082.75	0.25			
JMA	Oct. 1983 ... Dec. 1995	45605.0 ... 45672.5	0.5	Analysis-phase data	10 hPa	On real mountains
		45680.25 ... 46611.25	1.0			
		46612.0 ... 48794.0	0.5			
		48794.00 ... 50082.75	0.25			

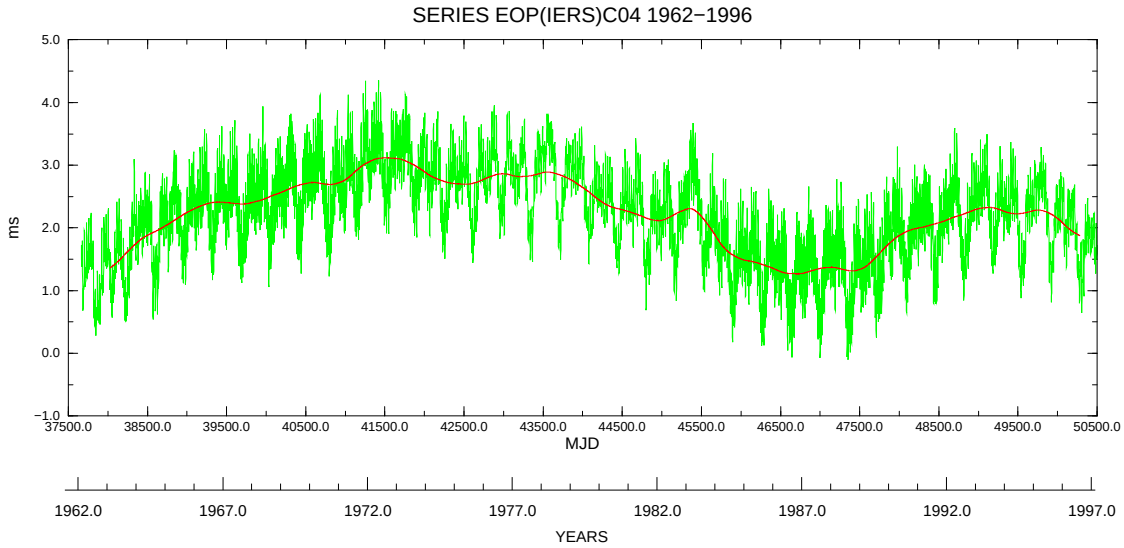

Figure 5. Length-Of-Day variation as computed as a combined solution by the IERS defined to be LOD. Note its trend showed as smooth line

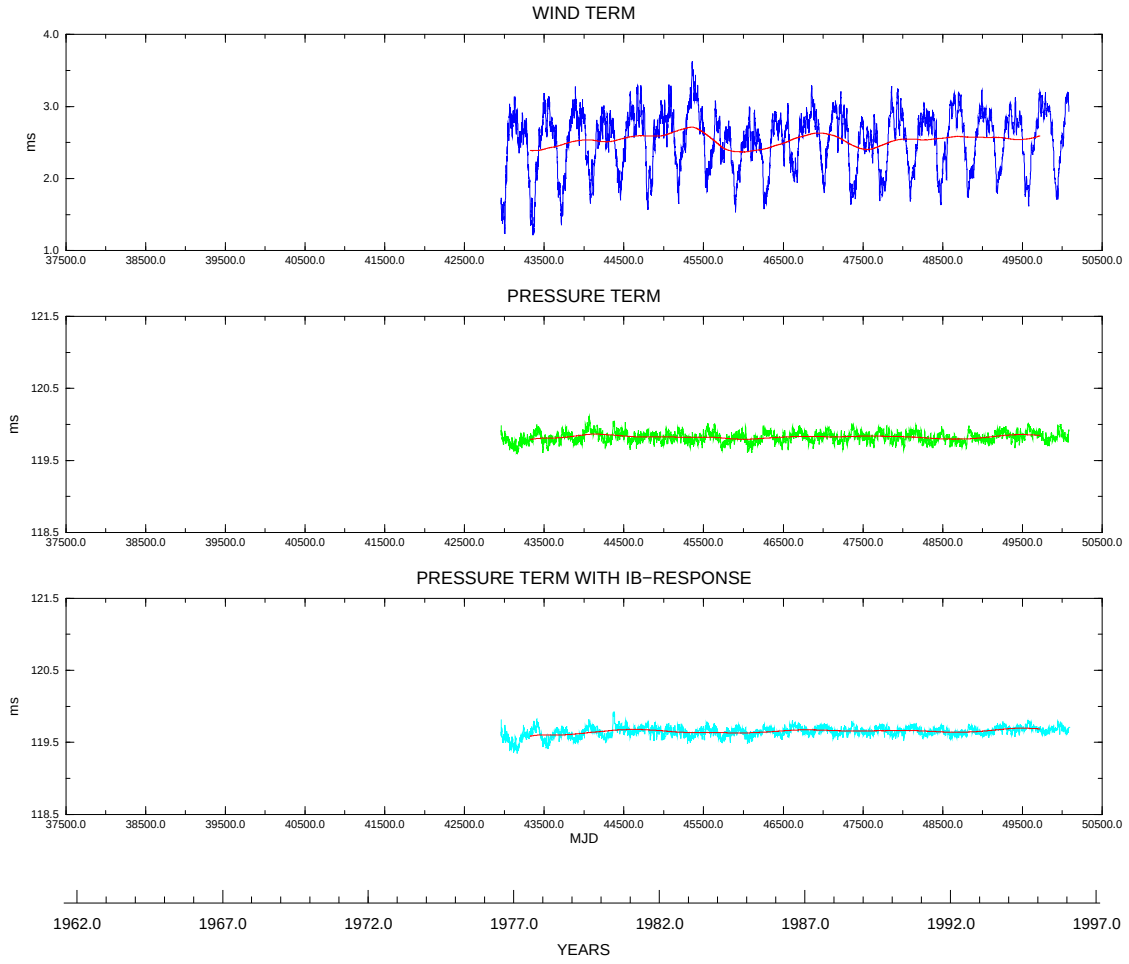

Figure 6. Length-Of-Day variations as inferred by Atmospheric-Angular-Momentum computed by the NMC defined to be $\mathrm{LOD}_{\mathrm{atm}}$: Wind term χ_3(W) (top), pressure term χ_3(P) (centre) and pressure IB term χ_3(P+IB) (bottom). Note: Each together with its trend

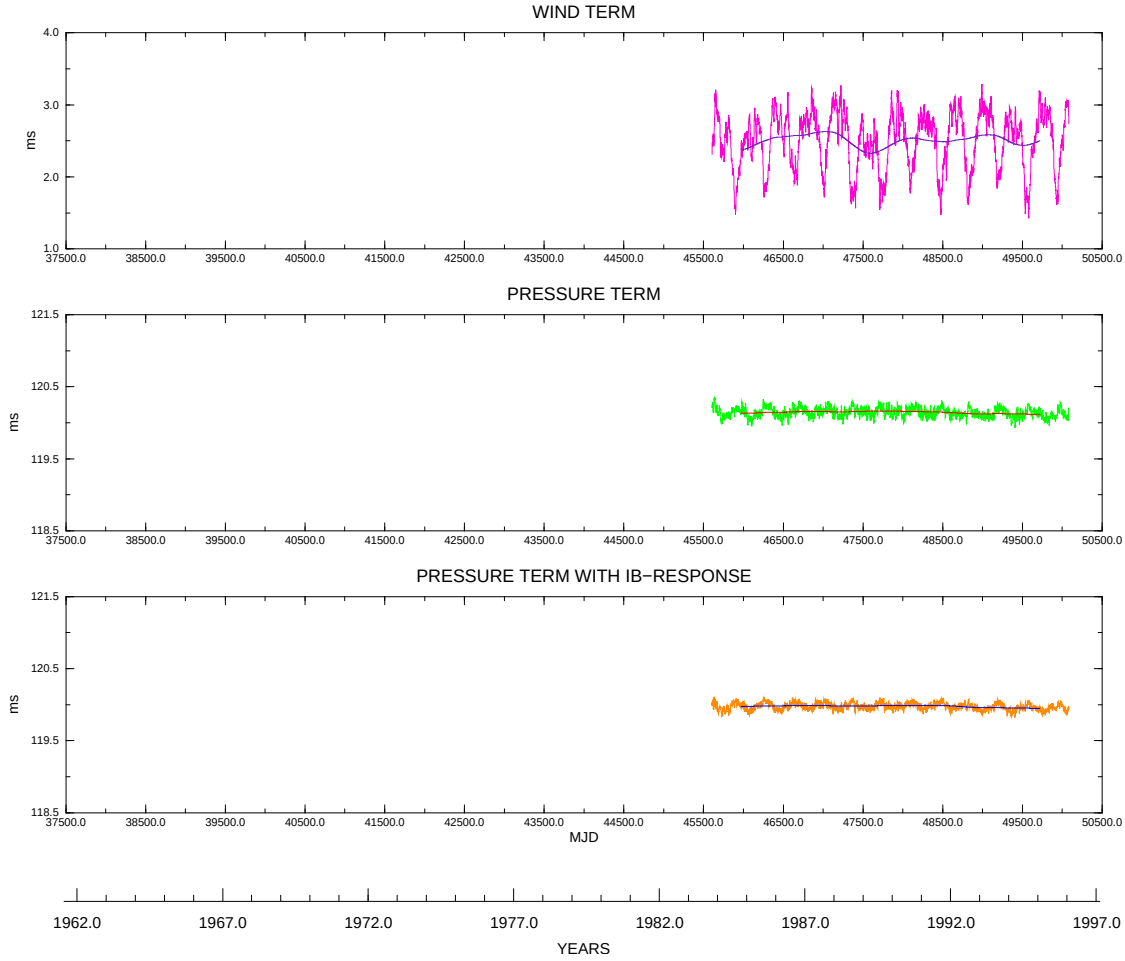

Figure 7. Same as Fig. 6, but computed by the JMA

3.2 AAM series

In general, the Earth rotation variations can be excited by two different terms: The mass term associated with mass redistribution outside or within the solid Earth that changes the Earth's inertia tensor, and the motion term associated with movement that carries net relative angular momentum. Concerning the atmospheric excitation, as noted earlier, the effective Atmospheric-Angular-Momentum functions related to Earth rotation are described by Barnes et al. (1983). The equatorial components χ_1 and χ_2 are related to the excitation of the polar motion, and the axial component χ_3 is related to changes in LOD. According to the two excitation origins, they are partitioned into contributions by wind and pressure that will be called motion term or wind term and matter term or pressure term, respectively. The AAM values have been calculated from forecast and analysis data sets for numerical weather prediction, and they are available from the four meteorological analysis centers: NMC, UKMO, JMA, and ECMWF. The abbreviations used to denote these are as in Section 2.

The forecast and analysis system used at the major weather centers is a complex three-step cycle including analysis, initialization and forecast. Consequently, there are three kinds of data: the analysis-phase data, the initialized-phase data, and the forecast data. For computing AAM functions, the NMC, UKMO and ECMWF source data are the initialized-phase data, while the JMA estimates are based on the analysis-phase data. The analysis step assimilates all raw meteorological observations from the heterogeneous network of upper-air radiosondes, aircraft, and a variety of satellite-based observing systems. Its results are a set of mean surface pressure over the globe and a set of global wind fields on a 2.5 x 2.5 degree latitude-longitude grid at the surface and different standard pressure levels in the vertical. As reported in IERS (1995), there are now 12 mandatory levels, namely at 1000, 850, 700, 500, 400, 300, 250, 200, 150, 100, 70 and 50 hPa. However, the computation of the analysis-phase data varies over the depth of the atmosphere in the global circulation models of the analysis centers. For example, the JMA produces the data set at 15 levels up to 10 hPa. Since the top level of each analysis center varies (NMC: 50 hPa, UKMO: about 25 hPa, JMA: 10 hPa, and ECMWF: 10 hPa) the difference from the heights would be noticed in the strength of the seasonal cycle. For additional details, see, e. g., Salstein and Rosen (1985); Naito, Kikuchi and Yokoyama (1987); Salstein et al. (1993); IERS (1995).

As noted above, we are here only concerned with the axial component χ_3 and in particular with the wind term labelled χ_3(W) and with the pressure term computed under two idealized extremes: without and with inverted barometer effect labelled χ_3(P) and χ_3(P+IB), respectively. χ_3(W) is the dominant term in AAM and must be evaluated from the global zonal wind speed at all fixed altitudes. Compared to χ_3(W), the pressure terms χ_3(P) and χ_3(P+IB) are relatively small. The non-IB case assumes zero yielding of the ocean to air pressure loading, whereas in the IB case the ocean responds to the changing loading and unloading completely isostatically. The reality presumably lies somewhere between the two extreme cases of non-IB and IB. The two weather centers NMC and JMA calculate both types of the pressure terms, whereas the other two centers do not so. The accurate determination of the oceanic contribution to the pressure term requires a model of the dynamic response more sophisticated than that of the inverted barometer model.

Concerning the calculation of the pressure term, it should be noted that the values based on the NMC and ECMWF data are computed directly from the initialized surface pressures on the model-mountains, while those based on the JMA data are estimated using the surface pressures on the real mountains re-estimated from the geopotentials and temperatures of the analysis-phase data (Naito et al. 1987).

The longest AAM series is the one computed by the NMC labelled AAM(NMC) since July 1976. There is also the AAM series computed by the JMA labelled AAM(JMA) since October 1983. Related to LOD, the data sets used to derive the seasonal oscillations are the following time series of the two types: χ_3(W), χ_3(P) and χ_3(P+IB) of the series AAM(NMC) from July 1, 1976 to December 31, 1995, i. e. MJD from 42960.0 to 50082.0, and χ_3(W), χ_3(P) and χ_3(P+IB) of the series AAM(JMA) from September 28, 1983 to December 31, 1995, i. e. MJD from 45605.0 to 50082.0. Table 4 lists some characteristics of the AAM data used here.

As can be seen, the AAM data are typically produced on the basis of an increased sample over time. Also note that those of JMA sampled daily (i. e. from December 11, 1983 to June 30, 1986) are provided at 6 h UTC. Earlier data generally have less complete coverage in the altitude, often leaving out the entire stratosphere or a large portion of it. Hence, before January 1981, the NMC data cover the altitude only up to the 100 hPa level (altitude of about 16 km), encompassing 90 per cent of the mass of the atmosphere. The calculated AAM routinely then incorporate data at levels up to the 50-hPa level (about 21 km). In contrast, the JMA data integrate winds from the surface up to the 10-hPa level (about 30 km), accounting for 99 per cent of the atmosphere in terms of mass. Regarding the data homogeneity, it should be noticed that due to substantial changes in the general circulation models used to assimilate the original meteorological observations, the NMC data are less homogeneous than those of JMA.

On the assumption that changes in the angular momentum of the entire atmosphere about the polar axis relative to an Earth-fixed frame are accompanied by equal, but opposite, changes in the Earth's angular momentum, we have

$$\mathrm{LOD}_{\mathrm{atm}} = -\chi_3 \,, \tag{1}$$

Table 5. Estimates of the correlation coefficient *r* between LOD and $\mathrm{LOD}_{\mathrm{atm}}$ series

System	Period (in MJD)	Number of values	r (LOD, $\mathrm{LOD}_{\mathrm{atm}}$) with $\mathrm{LOD}_{\mathrm{atm}} = -\chi_3$		LOD original data Expectation values as computed trend		LOD data without the tides Sa and Ssa Expectation values as computed trend	
NMC	43325.0 ... 49717.0	6393		χ_3(W)		+0.71687		+0.73147
			χ_3(P)	+ χ_3(W)	-0.22551	+0.72588	-0.24388	+0.73810
			χ_3(P+IB)	+ χ_3(W)	-0.28673	+0.72597	-0.30829	+0.73836
JMA	45970.0 ... 49717.0	3748		χ_3(W)		+0.69647		+0.70649
			χ_3(P)	+ χ_3(W)	-0.22257	+0.70297	-0.23582	+0.71128
			χ_3(P+IB)	+ χ_3(W)	-0.31057	+0.70292	-0.32081	+0.71231

where $\mathrm{LOD}_{\mathrm{atm}}$ are the atmospheric contributions to LOD, i. e. LOD inferred from AAM. Units of the AAM data are non-dimensional, while LOD is expressed in seconds of time (s). Thus, the AAM are converted into $\mathrm{LOD}_{\mathrm{atm}}$ estimates by inverting their signs and multiplying by the scale factor of 8.64 x 10^4.

Preparatory to further analysis of the $\mathrm{LOD}_{\mathrm{atm}}$ data, it is necessary to produce time series free of gaps as well as random and systematic errors and to make available evenly spaced daily series. Gaps as found by testing the sampling intervals were removed as follows: First, occasional gaps were linearly interpolated. Then, those of a few days were filled by making use of the data of the other weather centers or by a more sophisticated interpolation method. Changes in atmospheric circulation models lead to systematic errors in the form of step-like discontinuities in the time series. Some jumps were found with a few gross errors by visualizing the different sets. We removed each resultant discontinuity by simply subtracting the difference between the values on this date from all either earlier or subsequent values. The step jumps found and removed in the pressure terms χ_3(P) and χ_3(P+IB) of NMC system are on August 18, 1976 (MJD 43008), on May 1, 1980 (MJD 44360), on May 28, 1986 (MJD 46579), on August 12, 1987 (MJD 47020) and on March 5, 1991 (MJD 48321) of which two are mentioned in Rosen, Salstein and Wood (1990). In case of the detected outliers, the linear interpolation was usually applied. The one-day JMA series with MJD from 45680.25 to 46611.25 had to be resampled using linear interpolation to conform to sampling at the epochs 0 and 12 h UTC. After pre-processing the AAM data in the described manner, the NMC and JMA $\mathrm{LOD}_{\mathrm{atm}}$ series at daily intervals over their entire time spans were used as input data for this study together with those of LOD.

Concerning the uncertainties of the AAM time series, the following should be noted: None of the weather centers that compute these data give uncertainty estimates. However, there are a number of studies done to assess the errors of AAM, especially for the wind term χ_3(W) (see, e. g., Eubanks et al. 1985b; Rosen et al. 1987). They are primarily based on a comparison of the time series of the various weather centers with each other. It shows that the mean intercenter difference between χ_3(W) estimates on a calendar year basis has diminished considerably in recent years (Rosen 1993). From these and own studies, Freedman et al. (1994) chose a nominal value of 0.05 ms as the formal error for the NMC AAM analysis and forecast series. As reported in Naito and Kikuchi (1990), in general, the χ_3(W) computed by JMA have an error around 3%. Computing the pressure terms χ_3(P) and χ_3(P+IB) from the operational analyses is somewhat more problematic than computing the wind term χ_3(W), as is evident by step jumps that correspond on occasions to procedural changes. The error in the pressure term is comparable to that in the wind term during a period assessed by comparison of NMC and ECMWF χ_3(P) values (Rosen et al. 1990).

The $\mathrm{LOD}_{\mathrm{atm}}$ data sets of the NMC system are displayed in Fig. 6 and those of the JMA system in Fig. 7. For purposes of comparison, the series have been plotted on the same time scale as the LOD in Fig. 5. The three curves are the variations of the wind term χ_3(W) at the top, the pressure term χ_3(P) at the centre, and the pressure IB term χ_3(P+IB) at the bottom. The trends found by applying a low-pass filter to the six data sets are illustrated as well. Details of the filtering procedure can be found in Section 5. In Figs 6 and 7, notice the strong similarities between the curves of the NMC and JMA systems, where the χ_3(W) plots are clearly dominated by the annual periodicity.

4 Correlations between LOD and $\mathrm{LOD}_{\mathrm{atm}}$ series

The correlation coefficient *r* between two data sets x = x_i and y = y_i with i = 1, 2, 3, ..., n is defined by the relation

$$r = \frac{\sum_{i=1}^{n}(x-\bar{x})(y-\bar{y})}{\sqrt{\sum_{i=1}^{n}(x-\bar{x})^2 \sum_{i=1}^{n}(y-\bar{y})^2}} , \qquad (2)$$

where $\bar{x}$, $\bar{y}$ are the expectation values, i. e. the trend values of x and y, respectively, in case of time series, and n is the number of values in each series, i. e. the sample size. The result is a dimensionless measure ranging from -1 to +1. it means:

(a) If r = 0, then there is no correlation between x and y;
(b) if r = +1, then the correlation is strict like;
(c) if r = -1, then the correlation is strict opposite.

Consequently, the correlation coefficient *r* is a measure that shows the strength of linear correlation between two variables, and is, for that reason, extensively used in data analysis as a rough measure of intervariable relationship.

To obtain a first idea of the relationship between the LOD and $\mathrm{LOD}_{\mathrm{atm}}$ time series, their correlations have been computed using formula (2). Table 5 gives the estimates of the correlation coefficient r for the NMC and JMA systems, where the trends and the attached periods are those of the trend calculations, see Section 5 and compare with Figs 5, 6 and 7. Especially in the $\mathrm{LOD}_{\mathrm{atm}}$, we included the wind term and the two pressure terms separately and jointly. Furthermore, we produced similar results from LOD data from which the tidal effects Sa and Ssa were removed.

The above correlation estimates are clearly depending on the sample size. It should be noted that they are average values over the periods considered and that the correlation may be time-variable. Presumably degraded by systematic errors in the AAM(NMC) series, the correlation coefficient *r* is somewhat lower in earlier years.

For the wind term χ_3(W), we have a correlation estimate of about +0.7. Then, it is interesting to see that the correlation coefficient is about -0.2 for the pressure term χ_3(P) and about -0.3 for the pressure IB term χ_3(P+IB). After combining the wind term χ_3(W) with the pressure term χ_3(P) and χ_3(P+IB), respectively, the correlations are somewhat higher than that for the wind term χ_3(W) alone. Indeed, the IB effect produces not a significantly higher correlation estimate than the non-IB case. Regarding the LOD data without the tidal oscillations Sa and Ssa, it can be noticed that they consistently yield higher correlation estimates than the original LOD data.

Some preliminary interpretations are as follows: Although the pressure term itself is more than an order of magnitude smaller than the wind term, it may also play a role. The consideration of the χ_3(P) and χ_3(P+IB) data, respectively, in the χ_3(W) series has a counterbalance effect. Therefore, very likely, there is better agreement between the seasonal oscillations of the LOD and $\mathrm{LOD}_{\mathrm{atm}}$ series if the latter include both wind and pressure terms. For purposes of comparison, it is recommended that the tidal effects Sa and Ssa have been removed from the seasonal oscillations of LOD.

5 Data analysis

To focus on the seasonal discrepancies between LOD and $\mathrm{LOD}_{\mathrm{atm}}$ series, we applied two analysis steps:

(a) Separating the major components by filtering the time series:

Using one-day values, the data are analyzed for the following periods:
- LOD from January 1, 1962 to June 11, 1996, i. e. MJD from 37665.0 to 50245.0,
- $\mathrm{LOD}_{\mathrm{atm}}$ of the NMC system from July 1, 1976 to December 31, 1995, i. e. MJD from 42960.0 to 50082.0,
- $\mathrm{LOD}_{\mathrm{atm}}$ of the JMA system from September 28, 1983 to December 31, 1995, i. e. MJD from 45605.0 to 50082.0.

By using filters the filtered series are truncated at either end of the analysis period as explained for the seasonal oscillations in (b). For more details, see Section 5.1.

(b) Calculating optimal estimates of the parameters of the seasonal oscillations:

Using one-day values, the data are analyzed for the following periods:
Annual oscillation of
- LOD from March 5, 1964 to April 9, 1994, i. e. MJD from 38459.0 to 49451.0,
- $\mathrm{LOD}_{\mathrm{atm}}$ of the NMC system from September 3, 1978 to October 28, 1993, i. e. MJD from 43754.0 to 49288.0,
- $\mathrm{LOD}_{\mathrm{atm}}$ of the JMA system from November 30, 1985 to October 28, 1993, i. e. MJD from 46399.0 to 49288.0.

Semiannual oscillation of
- LOD from January 29, 1963 to May 15, 1995, i. e. MJD from 38058.0 to 49852.0,
- $\mathrm{LOD}_{\mathrm{atm}}$ of the NMC system from July 29, 1977 to December 3, 1994, i. e. MJD from 43353.0 to 49689.0,
- $\mathrm{LOD}_{\mathrm{atm}}$ of the JMA system from October 25, 1984 to December 3, 1994, i. e. MJD from 45998.0 to 49689.0.

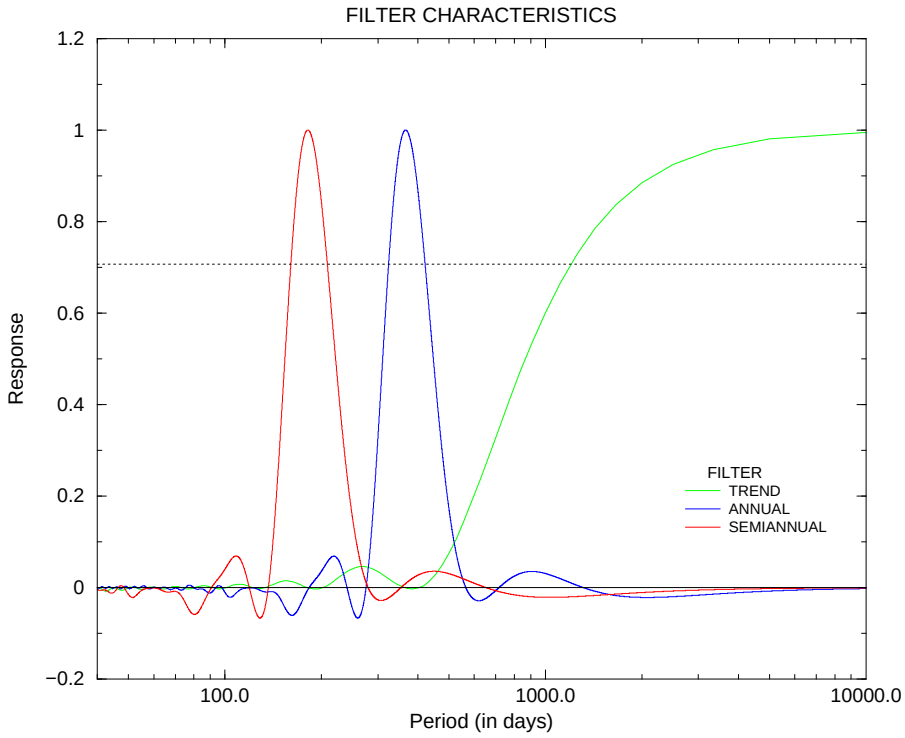

Figure 8. Amplitude characteristics of the filters as applied for separating the trend as well as the annual and semiannual oscillations from the original time series. Note: Response is given as function of period. Half-power points are the points of intersection between each curve and the horizontal light dotted line

5.1 Filtering the time series

As reported in Höpfner (1996), we have designed zero-phase digital filters for separating the major components from the original data at one-day intervals. These filters were applied to the LOD and $\mathrm{LOD}_{\mathrm{atm}}$ series. Before describing the results, some information about the filters is given:

The low-pass filter to isolate the long-term trend is a 731-point filter. For separating the annual and semiannual oscillations, the band-pass filters are a 1589-point and a 787-point filter, respectively. To exhibit the amplitude characteristics of the filters, we computed the response function for each filter in terms of the ratio of the amplitude of fluctuations after filtering to that before. They are depicted in Fig. 8, contrary to Höpfner (1996) not as functions of frequency but as those of period. The low-pass filter used here has a cut-off period of 415 days. Regarding the half-power points of both band-pass filters, it should be noted that these are at approximately 324 and 421 days for the annual oscillation and at approximately 160 and 208 days for the semiannual oscillation. In Fig. 8, they are shown by the points of intersection between each response curve and the horizontal light dotted line.

One advantage of the filtering technique is its simple use. Because of constructing zero-phase filters, these do not introduce lags or leads into the filtered data. Furthermore, the different components are well filtered out from the input data. The drawback is that the filtered series are truncated at the beginning and at the end of the analysis interval. The number of values lost at either end are 365 estimates of the trend series, 794 of the annual oscillation series and 393 of the semiannual oscillation series.

To separate a long-term trend from the original LOD data, this series is first low-pass filtered. The $\mathrm{LOD}_{\mathrm{atm}}$ data sets of the NMC and the JMA systems, either including the wind term χ_3(W), the pressure term χ_3(P) and the pressure IB term χ_3(P+IB) series, are then processed in a similar manner to the LOD data. As mentioned above, the LOD variation together with its trend is shown in Fig. 5; see Section 3.1. Moreover, the $\mathrm{LOD}_{\mathrm{atm}}$ series and their trends for both systems are plotted in Figs 6 and 7, see Section 3.2. For using the trends in computations of correlations between LOD and $\mathrm{LOD}_{\mathrm{atm}}$, see Section 4. The LOD data have a long-term drift, not matched by the $\mathrm{LOD}_{\mathrm{atm}}$ data. This is probably the result of a core-mantle angular momentum exchange, as reported earlier; see, e. g., Lambeck (1980); Eubanks et al. (1985b); Greiner-Mai (1993, 1995).

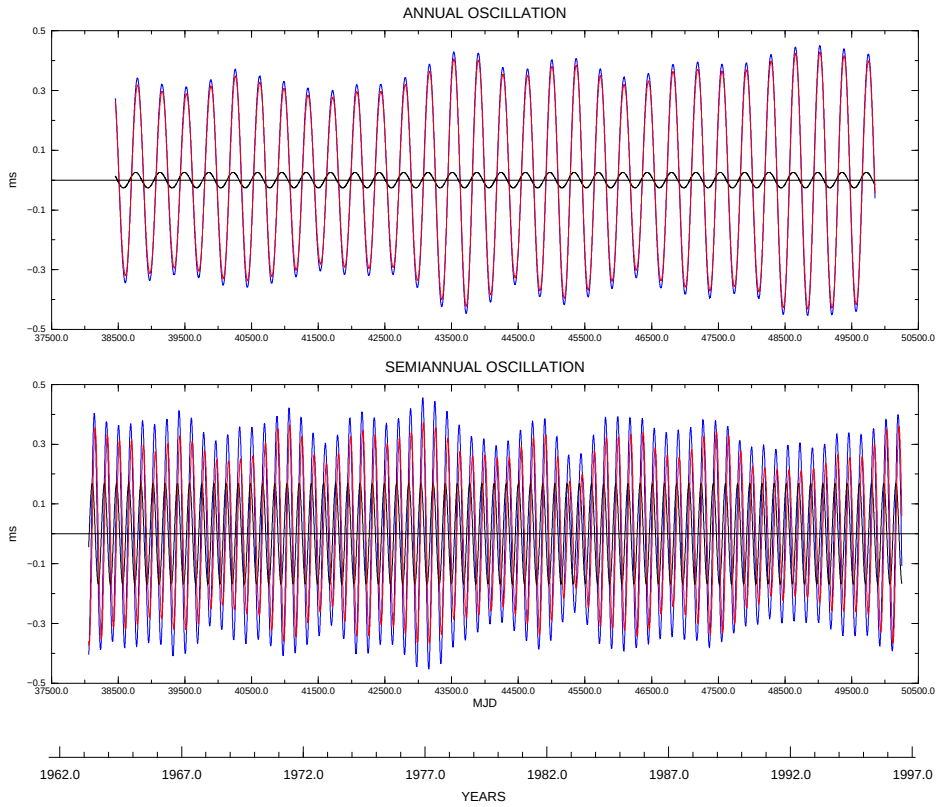

Figure 9. Top: Annual oscillation in the LOD variation with and without tidal effect Sa as well as the tidal effect Sa. Bottom: Semiannual oscillation in the LOD variation with and without tidal effect Ssa as well as the tidal effect Ssa. In both cases, the LOD oscillation with tidal effect is plotted in blue, that without tidal effect in red and the tidal effect in black

Band-pass filtering was used to isolate the annual and semiannual oscillations in the LOD data. Since the tidal effects Sa and Ssa induced by the tides of the solid Earth and oceans still contribute to the seasonal oscillations of LOD, they have been removed by adopting IERS Standards (McCarthy 1992) according to Yoder, Williams and Parke (1981) modified by the ocean effects derived from Dickman (1991). In Fig. 9, the annual oscillation of LOD with and without the tidal effect Sa is shown at the top and the semiannual oscillation with and without the tidal effect Ssa at the bottom. Also displayed are the two tidal effects themselves. In the same manner as for the LOD data, the $\mathrm{LOD}_{\mathrm{atm}}$ series of the NMC and JMA systems were filtered by the two band-pass digital filters. The resulting annual and semiannual oscillations are illustrated in Figs 10 and 11, respectively, for the NMC system, and in Figs 12 and 13, respectively, for the JMA system. Here, the component of the wind term χ_3(W) is plotted at the top, the components of the pressure term χ_3(P) and of the wind plus pressure term χ_3(W) + χ_3(P) at the centre and those of the pressure IB term χ_3(P+IB) and of the wind plus pressure IB term χ_3(W) + χ_3(P+IB) at the bottom. It should be noted that the seasonal signals filtered out from the pressure term χ_3(P) and the pressure IB term χ_3(P+IB), although small, are well quantified and therefore clearly visible in Figs 10 to 13. As discussed earlier, incorporating both wind and pressure terms, the total seasonal signals of $\mathrm{LOD}_{\mathrm{atm}}$ should better coincide with those of LOD without the tidal effects Sa and Ssa.

5.2 Calculating optimal estimates of the oscillation parameters

As can be seen in Figs 9 to 13, the periodic signals of LOD and $\mathrm{LOD}_{\mathrm{atm}}$, respectively, change with time. Therefore, the objective was to obtain an optimal estimate of the three parameters of the seasonal oscillations: amplitude, period and phase. To quantify their temporal changes, we found it convenient to apply to the resulting data of the seasonal oscillations a simple method based on the maximum, zero passage and minimum of a periodic function instead of moving least-squares fits of annual and semiannual sinusoids, respectively, at quarterly intervals according to Höpfner (1996). The procedure involves the following successive steps:

(1) Searching the time series for its zero passages
(2) Finding the maxima and minima between the zero passages
(3) Forming the amplitude time series by inverting the signs of the minima, where the estimates may be called plus- and

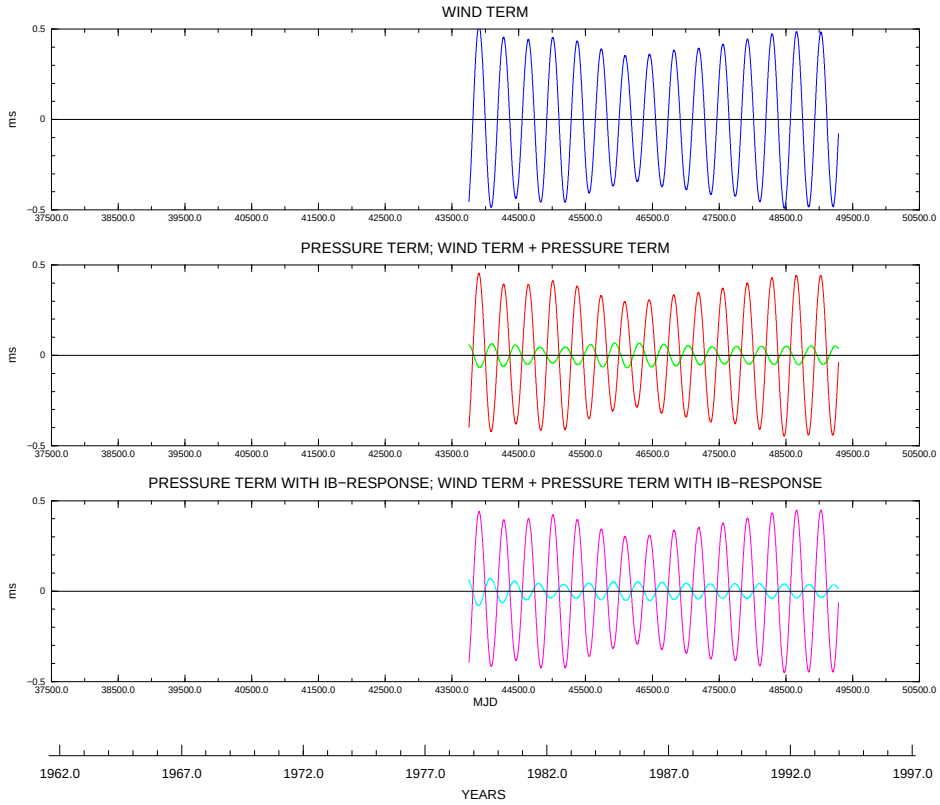

Figure 10. Annual oscillation of the $\mathrm{LOD}_{\mathrm{atm}}$ variations of the NMC system: Component of the wind term χ_3(W) (top), components of the pressure term χ_3(P) and of the wind plus pressure term χ_3(W) + χ_3(P) (centre) and those of the pressure IB term χ_3(P+IB) and of the wind plus pressure IB term χ_3(W) + χ_3(P+IB) (bottom)

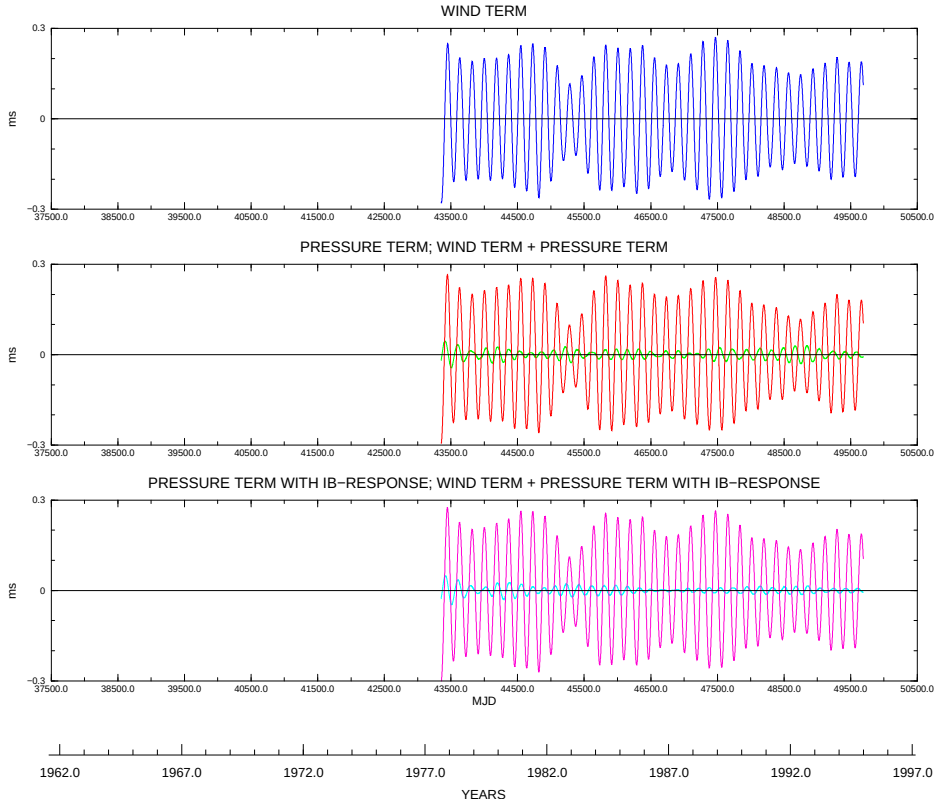

Figure 11. Same as Fig. 10, but for the semiannual oscillation of the $\mathrm{LOD}_{\mathrm{atm}}$ variations of the NMC system

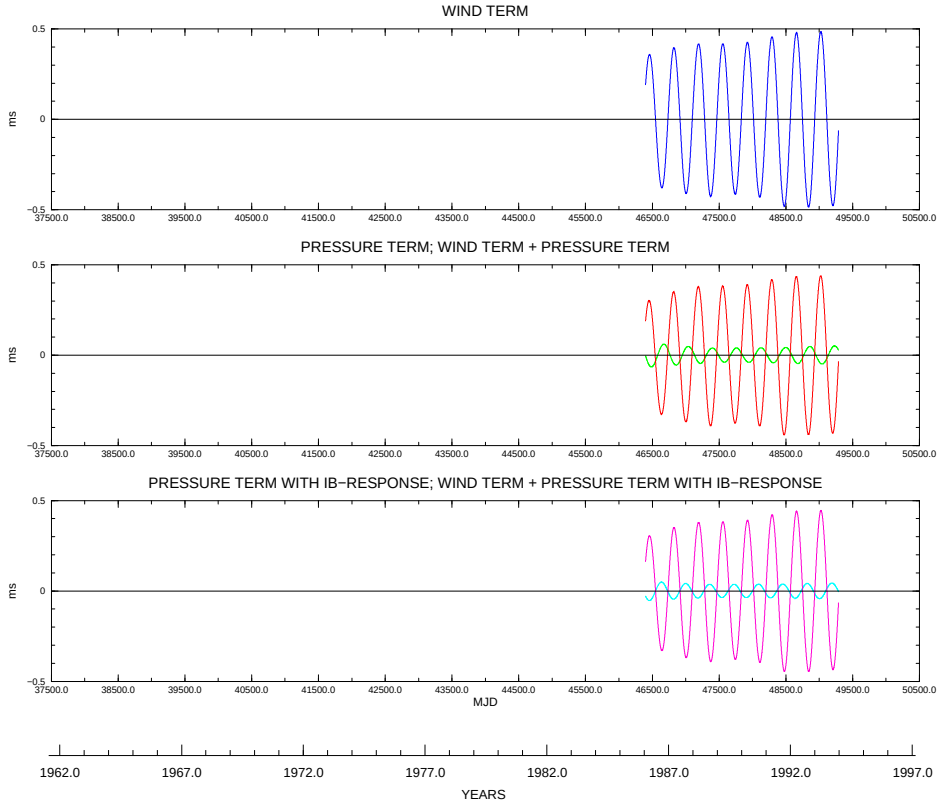

Figure 12. Same as Fig. 10, but for the annual oscillation of the $\mathrm{LOD}_{\mathrm{atm}}$ variations of the JMA system

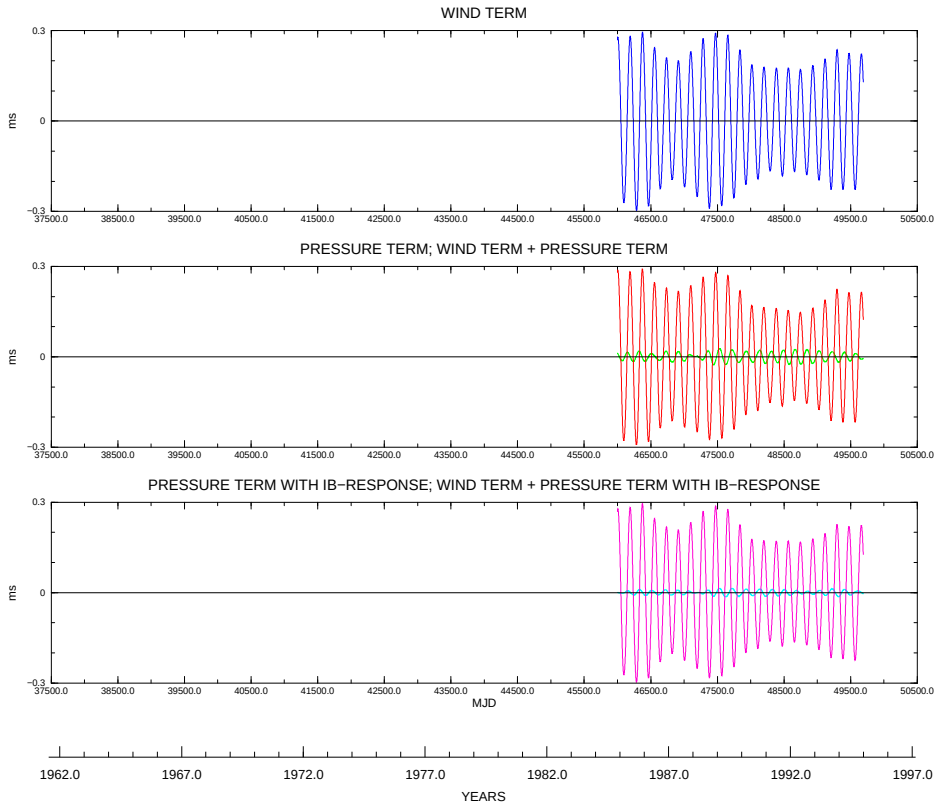

Figure 13. Same as Fig. 10, but for the semiannual oscillation of the $\mathrm{LOD}_{\mathrm{atm}}$ variations of the JMA system

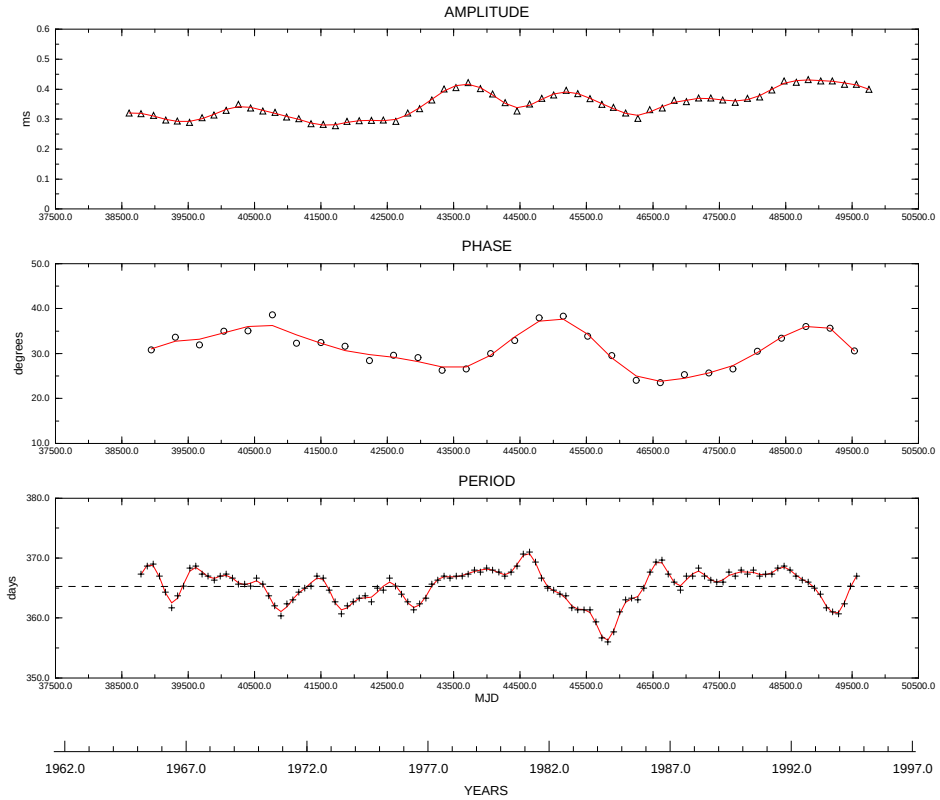

Figure 14. Parameter variability with time of the annual oscillation of LOD without tidal effect Sa: Amplitude (top), phase (centre) and period variation (bottom). Note: The distinctive markers indicate the estimates where triangles are used for the plus-and minus-amplitude values, circles for the means from plus- and minus-phase values and crosses for the moving three-point means from plus-, zero- and minus-period values. The curves show the estimates derived from a 5-point smoothing

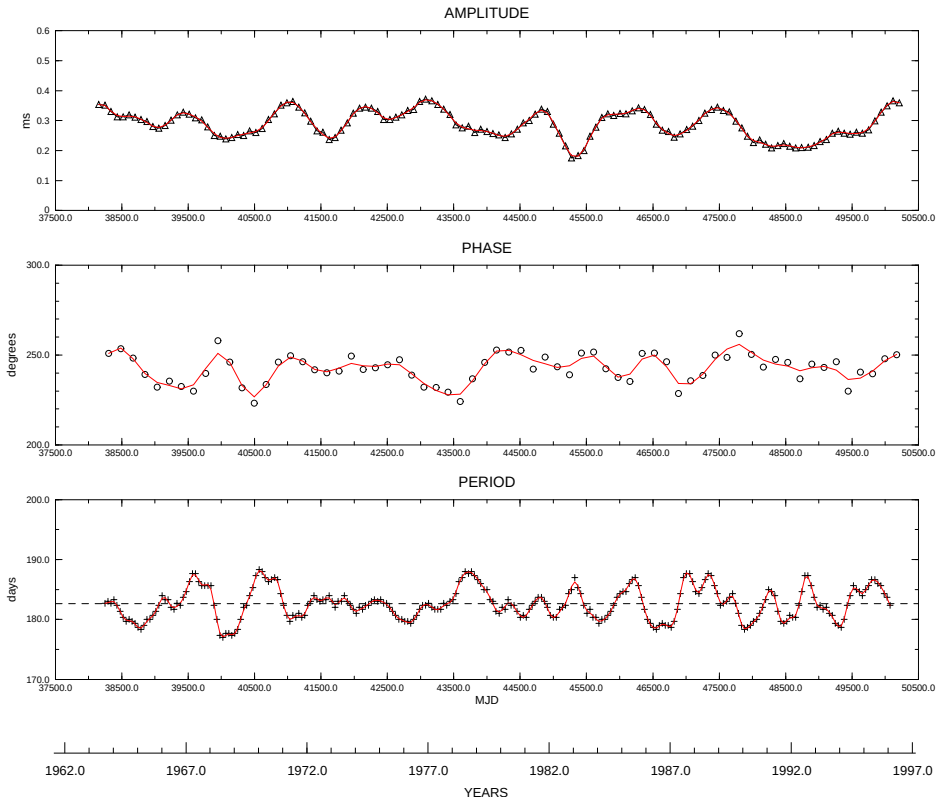

Figure 15. Same as Fig. 14, but for the semiannual oscillation of LOD without tidal effect Ssa

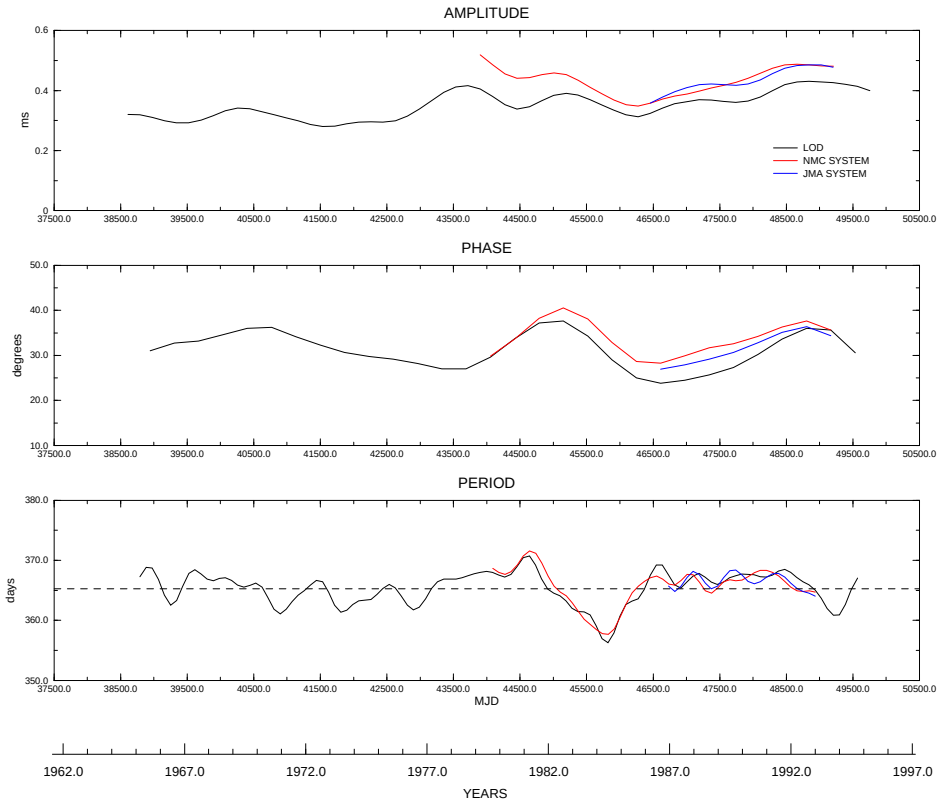

Figure 16. Parameter variability with time of the annual oscillation in LOD and $\mathrm{LOD_{atm}}$: Amplitude (top), phase (centre) and period variation (bottom) of the component of LOD without the tidal effect Sa and of the wind terms χ_3(W) in the NMC and JMA systems. Note: The curves are showing the estimates derived from a 5-point smoothing

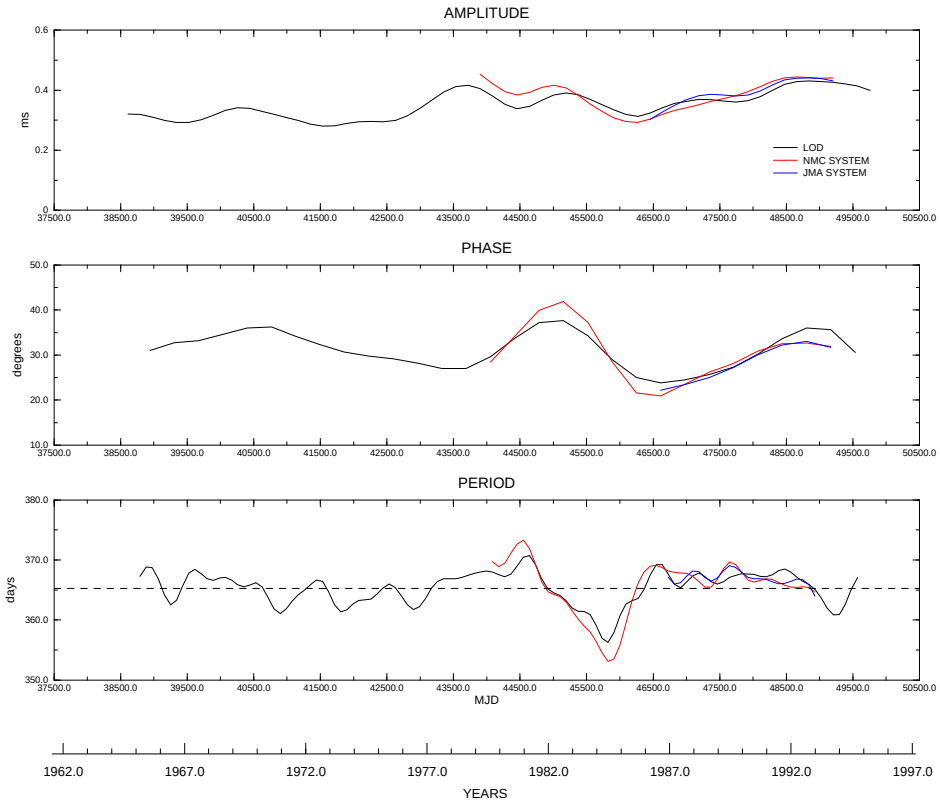

Figure 17. Same as Fig. 16, but for the wind plus pressure terms χ_3(W) + χ_3(P)

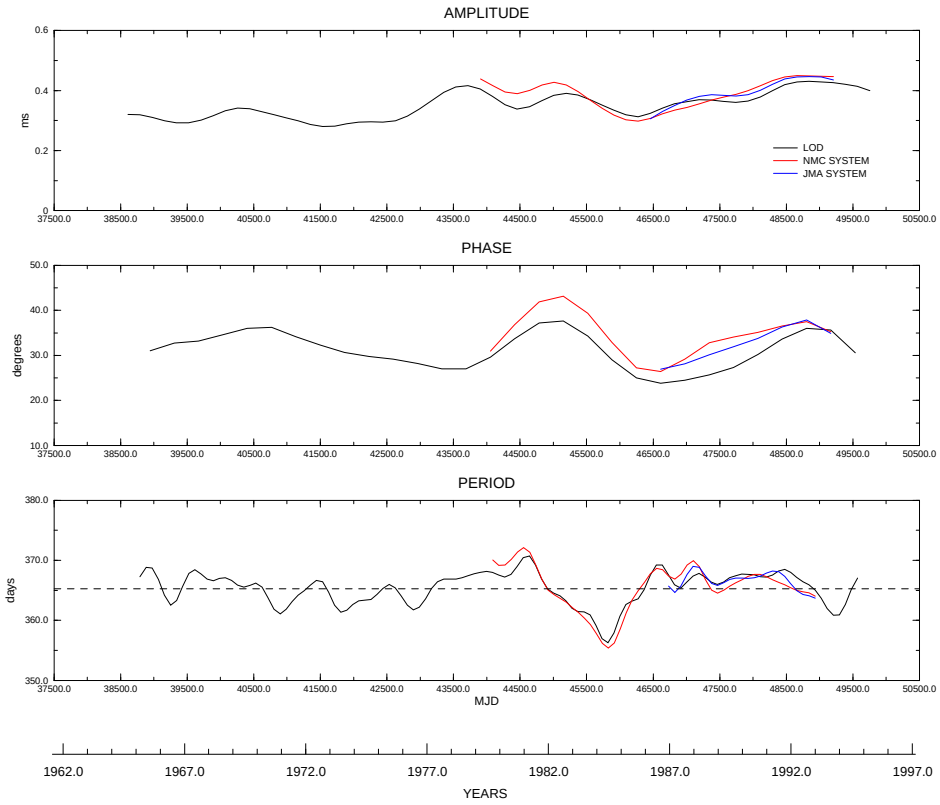

Figure 18. Same as Fig. 16, but for the wind plus pressure IB terms χ_3(W) + χ_3(P+IB)

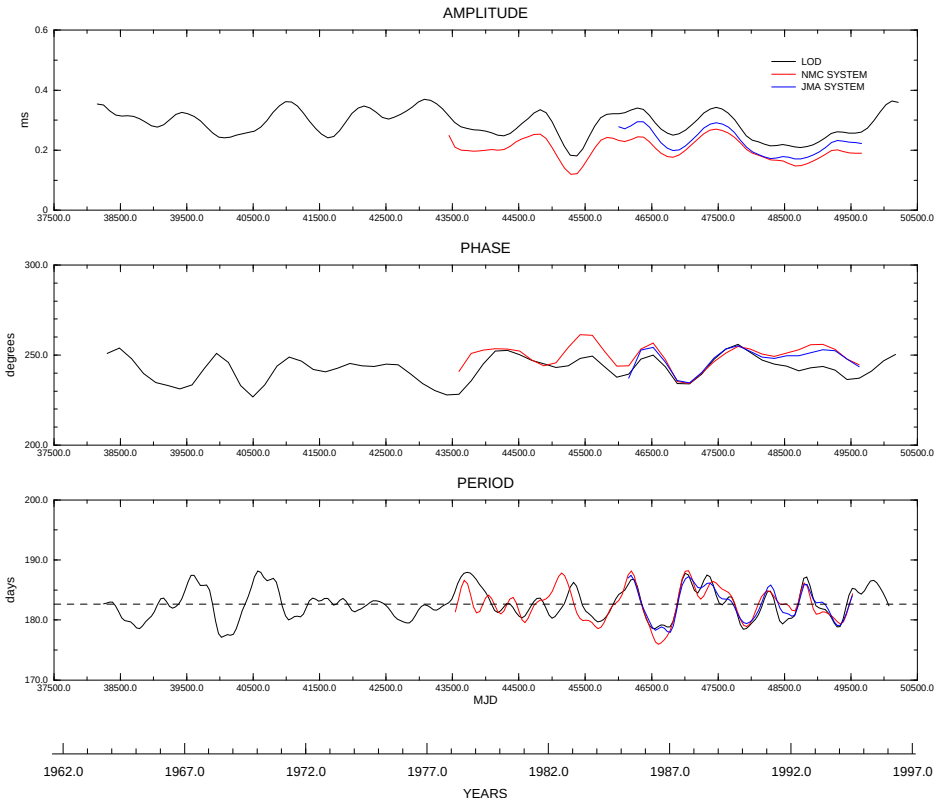

Figure 19. Parameter variability with time of the semiannual oscillation in LOD and $\mathrm{LOD_{atm}}$: Amplitude (top), phase (centre) and period variation (bottom) of the component of LOD without the tidal effect Ssa and of the wind terms χ_3(W) in the NMC and JMA systems. Note: The curves show the estimates derived from a 5-point smoothing

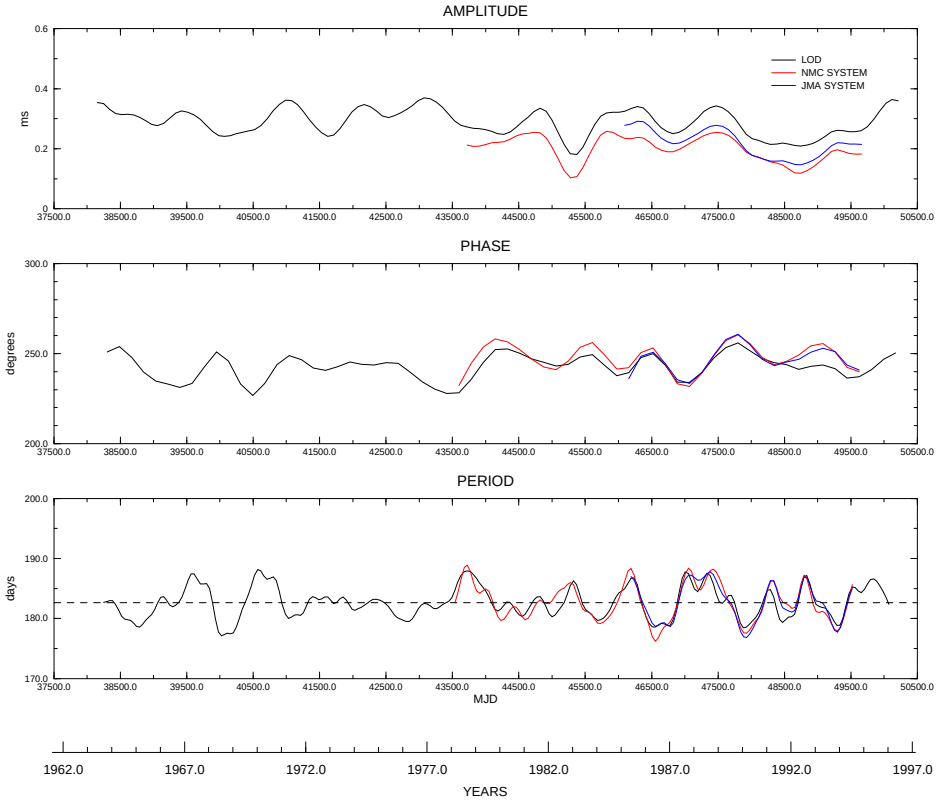

Figure 20. Same as Fig. 19, but for the wind plus pressure terms χ_3(W) + χ_3(P)

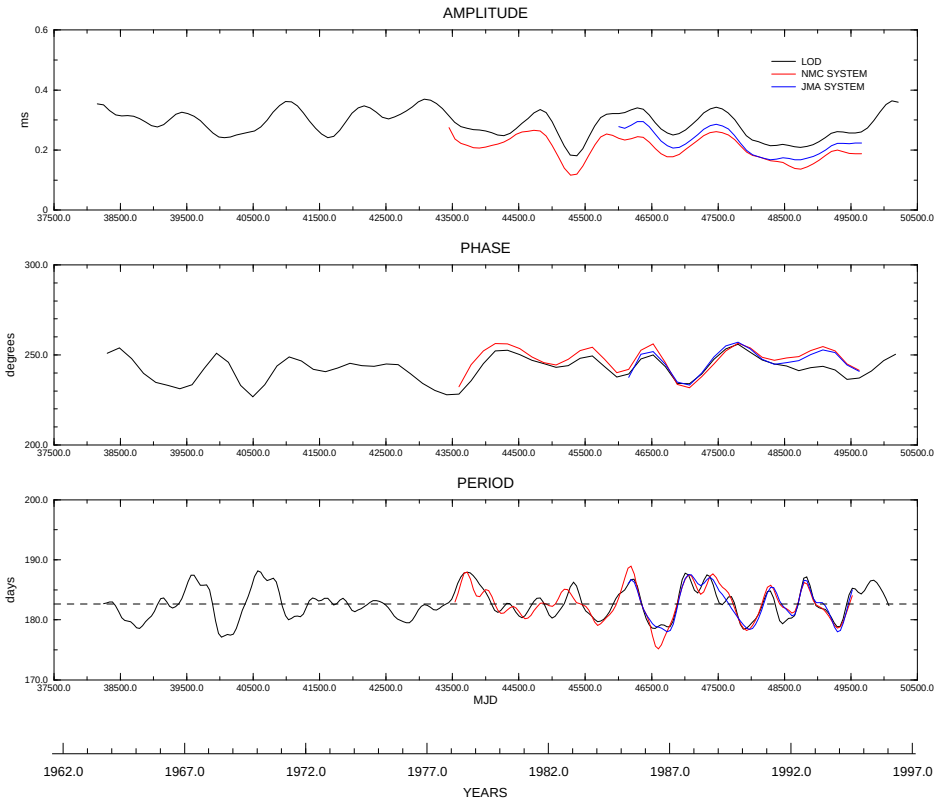

Figure 21. Same as Fig. 19, but for the wind plus pressure IB terms χ_3(W) + χ_3(P+IB)

minus-amplitudes
(4) Finding out the period values as moving three-point means, each from two successive maxima called plus-period, from the zero passages in terms of double differences called zero-period, and from two successive minima called minus-period
(5) Determining the phase angles as means, each from the difference between the beginning of a year / in case of the semiannual oscillation the middle of a year as well and the epoch of the maximum called plus-phase and the difference between the beginning of a year / in case of the semiannual oscillation the middle of a year as well and the epoch of the minimum called minus-phase, where both are first converted from days into degrees by making use of the attached interpolated period and the minus-phases are then reduced by 180^o.

As in Section 2, note that the phase angle refers to the cosine function, where the argument is expressed with negative phase value.

The sample standard deviation s_0 can be evaluated from double measurements by using the formula as, e. g., given in Großmann (1953)

$$s_0 = \pm\sqrt{\frac{\sum_{i=1}^{n} {d_i}^2}{2\,n}}\ , \tag{3}$$

where d_i are the differences between the measurements of the two series and n is the number of measurements in each series.

In case of our amplitude, period and phase-angle estimates of the oscillations at seasonal frequencies, the following should be noted for applying formula (3) and computing the standard deviation of the mean from the uncertainty s_0:

(a) Amplitude time series
d_i are the differences between the absolute values of a successive maxima and minima, i. e. between the so-called plus- and minus-amplitudes. Consequently, n is the number of pairs of the extreme estimates in a series. Here, the standard deviation of the mean is given by $s_{\mathrm{amplitude}} = s_0 / \sqrt{2}$.

(b) Period time series
d_i are the moving differences among the successive so-called plus-period, zero-period and minus-period estimates. Consequently, n is the number of differences in a series. Here, the standard deviation of the moving three-point mean is given by $s_{\mathrm{period}} = s_0 / \sqrt{3}$.

(c) Phase-angle time series
d_i are the differences between the successive values of the so-called plus-phase at the maximum and the so-called minus-phase at the minimum (at the minus-phase considering a half period length by a phase change of 180^o). Consequently, n is the number of pairs of the plus- and minus-phase estimates in a series. Here, the standard deviation of the mean is given by $s_{\mathrm{phase}} = s_0 / \sqrt{2}$.

The procedure for deriving amplitude, period and phase changes may be shown by the example of the seasonal oscillations in LOD without the tidal effects Sa and Ssa. On the same scale as in earlier figures, the variability with time of the amplitude, phase and period of the oscillation at annual frequency is plotted in Fig. 14 and that at semiannual frequency in Fig. 15. We can be see the amplitude variation at the top, the phase variation at the centre and the period variation at the bottom of each figure. The period change has a reference baseline of 365.25 days for the annual oscillation and 182.625 days for the semiannual oscillation. Here, the estimates are denoted by distinctive markers, namely by triangles for the amplitude, by circles for the phase and by crosses for the period. They are smoothed with a moving 5-point average else. Figures 14 and 15 present these estimates in terms of curves. In the following figures, the display of parameter variability is restricted to this type of display. According to the described procedure, the seasonal $\mathrm{LOD}_{\mathrm{atm}}$ oscillations of the NMC and JMA systems were processed in a similar manner to those of the LOD data.

The LOD and $\mathrm{LOD}_{\mathrm{atm}}$ results obtained for the annual oscillation are illustrated in Figs 16 to 18 and those obtained for the semiannual oscillation in Figs 19 to 21. As for Figs 14 and 15, the amplitude variation is shown at the top, the phase variation at the centre and the period variation at the bottom of each figure. Strictly speaking:

(a) Annual frequency
Especially in Fig. 16, the three curves in each panel indicate the change of the parameters of the annual LOD component minus the tidal effect Sa and of the wind terms χ_3(W) in the NMC and JMA systems. The same as in Fig. 16 is shown

Table 6. Ranges of the variations of the amplitude, phase and period estimates of the seasonal oscillations in LOD and $\mathrm{LOD_{atm}}$. Min, minimum; Max, maximum; Dif, difference between maximum and minimum

Component	Period for IERS			Period for NMC			Period for JMA		
	Min	Max	Dif	Min	Max	Dif	Min	Max	Dif
(a) Annual oscillation									
Amplitude estimates (in ms)									
IERS LOD - Sa	0.273	0.432	0.159	0.289	0.432	0.142	0.334	0.432	0.098
NMC Wind				0.335	0.521	0.186	0.362	0.486	0.124
+ Pressure				0.280	0.457	0.177	0.307	0.442	0.135
+ Pressure + IB				0.285	0.447	0.162	0.311	0.447	0.136
JMA Wind							0.361	0.486	0.125
+ Pressure							0.305	0.440	0.135
+ Pressure + IB							0.309	0.446	0.137
Phase estimates (in degrees)									
IERS LOD - Sa	22.38	38.98	16.60	22.38	38.98	16.60	22.38	35.20	12.81
NMC Wind				26.85	40.76	13.91	26.85	36.82	9.97
+ Pressure				20.55	39.15	18.61	20.55	33.96	13.42
+ Pressure + IB				25.51	43.45	17.94	25.51	36.45	10.94
JMA Wind							27.41	34.85	7.44
+ Pressure							22.05	33.31	11.26
+ Pressure + IB							27.84	36.96	9.11
Period estimates (in days)									
IERS LOD - Sa	355.80	374.41	18.61	355.80	374.41	18.61	363.30	370.74	7.45
NMC Wind				354.68	371.00	16.33	363.07	369.71	6.65
+ Pressure				353.18	372.06	18.89	363.00	370.99	8.00
+ Pressure + IB				352.55	370.54	17.98	362.75	369.94	7.19
JMA Wind							363.41	370.53	7.12
+ Pressure							363.95	371.34	7.40
+ Pressure + IB							364.20	370.59	6.39
(b) Semiannual oscillation									
Amplitude estimates (in ms)									
IERS LOD - Ssa	0.175	0.372	0.197	0.175	0.344	0.169	0.209	0.344	0.136
NMC Wind				0.116	0.279	0.163	0.146	0.271	0.125
+ Pressure				0.098	0.295	0.197	0.116	0.257	0.141
+ Pressure + IB				0.111	0.303	0.192	0.136	0.264	0.128
JMA Wind							0.166	0.297	0.131
+ Pressure							0.145	0.292	0.147
+ Pressure + IB							0.162	0.297	0.135
Phase estimates (in degrees)									
IERS LOD - Ssa	226.30	256.96	30.65	228.21	256.96	28.75	232.68	256.96	24.28
NMC Wind				232.54	263.04	30.50	232.54	259.18	26.64
+ Pressure				231.65	261.02	29.37	231.65	261.02	29.37
+ Pressure + IB				231.13	257.94	26.81	231.13	257.94	26.81
JMA Wind							234.23	255.43	21.20
+ Pressure							232.41	261.09	28.68
+ Pressure + IB							232.19	257.88	25.69
Period estimates (in days)									
IERS LOD - Ssa	176.86	188.89	12.02	177.92	188.89	10.97	177.92	187.73	9.81
NMC Wind				176.05	188.18	12.13	176.05	188.18	12.13
+ Pressure				177.09	188.75	11.66	177.09	188.20	11.10
+ Pressure + IB				176.21	189.01	12.80	176.21	189.01	12.80
JMA Wind							177.90	187.51	9.60
+ Pressure							176.55	187.97	11.41
+ Pressure + IB							177.62	187.76	10.14

in Figs 17 and 18, but for the wind plus pressure terms χ_3(W) + χ_3(P) and the wind plus pressure IB terms χ_3(W) + χ_3(P+IB), respectively.

(b) Semiannual frequency
Figure 19 exhibits the variations of the parameters of the semiannual LOD component minus the tidal effect Ssa and of the wind terms χ_3(W) in the NMC and JMA systems. The same as in Fig. 19 is shown in Figs 20 and 21 but for the wind plus pressure terms χ_3(W) + χ_3(P) and the wind plus pressure IB terms χ_3(W) + χ_3(P+IB), respectively.

A survey of the range of the variations of the three parameters of the annual and semiannual components is displayed in Table 6, where the values are given not only for the periods of the calculation but also for short similar periods. For the different periods, see the introduction of Section 5 and particularly (b). Table 7 presents the standard errors of the estimates and means calculated as described above. The LOD and $\mathrm{LOD_{atm}}$ results are discussed in the next section. Note that LOD stands for LOD without the tidal effects Sa and Ssa in this and the following sections.

Table 7. Standard deviations of the amplitude, phase and period estimates of the seasonal oscillations in LOD and LODatm from double measurements. s_0, standard error of a single estimate; $s_{amplitude}$, standard error of an amplitude mean; s_{phase}, standard error of a phase mean; s_{period}, standard error of a period three-point mean; n, number of the pairs; in case of the period, number of the differences

Component	Amplitude			Phase			Period		
	s_0 (in ms)	$s_{amplitude}$ (in ms)	n	s_0 (in degrees)	s_{phase} (in degrees)	n	s_0 (in days)	s_{period} (in days)	n
(a) Annual oscillation									
IERS LOD - Sa	± 0.015	± 0.011	30	± 3.49	± 2.47	29	± 3.82	± 2.20	58
NMC Wind	0.014	0.010	15	1.85	1.31	15	2.18	1.26	28
+ Pressure	0.014	0.010	15	2.85	2.01	15	2.43	1.40	28
+ Pressure + IB	0.013	0.009	15	2.51	1.78	15	2.49	1.44	28
JMA Wind	0.008	0.006	8	1.23	0.87	8	1.48	0.85	13
+ Pressure	0.009	0.006	8	2.14	1.51	8	2.18	1.26	13
+ Pressure + IB	0.009	0.006	8	1.09	0.77	8	1.55	0.90	13
(b) Semiannual oscillation									
IERS LOD - Ssa	± 0.012	± 0.008	65	± 2.83	± 2.00	65	± 1.85	± 1.07	127
NMC Wind	0.011	0.008	35	2.70	1.91	35	1.41	0.81	67
+ Pressure	0.011	0.008	35	2.91	2.06	35	1.68	0.97	67
+ Pressure + IB	0.011	0.008	35	2.45	1.73	35	1.42	0.82	67
JMA Wind	0.011	0.008	20	2.68	1.89	20	1.24	0.71	38
+ Pressure	0.010	0.007	20	2.79	1.97	20	1.37	0.79	38
+ Pressure + IB	0.010	0.007	20	2.60	1.84	20	1.34	0.77	38

6 Discussion of the results

In the first place, it can be seen in Figs 14 to 21 and Tables 6 and 7 that all the seasonal components of LOD and of LOD_{atm} in the NMC and JMA systems show statistically significant variations of their amplitudes, phases and periods with time. Then, those derived from the LOD(IERS) series here agree well with those derived from the LOD(SLR) series reported by Höpfner (1996); compare Figs 14 and 15 with Figs 1 and 2, respectively. The LOD(SLR) series available for analysis was short and accordingly this comparison is restricted over short time spans, namely from 1986 to 1991 for the annual oscillation and from 1985 to 1992 for the semiannual oscillation. For reasons of space a direct comparison of the results is not given. As mentioned above, also note that the previous amplitudes, phases and periods are estimated by moving least-squares fits.

(a) Annual oscillation

Figure 16 (top) shows that the LOD amplitude estimates are typically smaller than those of the wind terms χ_3(W) of the NMC and JMA systems. The differences between those of LOD and those of the NMC system are larger at the beginning and decrease steady with time. There is an amplitude difference of about 0.05 ms. Over the JMA time interval, the amplitude variations of the wind terms χ_3(W) of both systems are rather similar, where the parallelism to those of LOD is better for those in the JMA system than for those in the NMC system. In Fig. 16 (centre), the phase-lag estimates of LOD differ from those of the wind term χ_3(W) of the NMC system by a few degrees at the beginning. If there exist those of the JMA system too, the differences among them are very small. Figure 16 (bottom) reveals that the annual period estimates of the three components vary in a corresponding manner, but the LOD period changes are obviously later for the JMA time span. The previous result of a period variation from 355 to 375 days is confirmed; see Höpfner (1996).

Compared to Fig. 16, it can be seen in Fig. 17 that the amplitude, phase and period variations of the wind plus pressure terms χ_3(W) + χ_3(P) of the NMC and JMA systems are quite similar with those for the wind terms χ_3(W) alone, i. e. the pressure term χ_3(P) produces no noticeable effect with time. However, there is a better agreement of these parameter estimates with the LOD estimates. In Fig. 17 (top), note the much smaller amplitude differences between both curves of the χ_3(W) + χ_3(P) NMC and JMA components and the curve of the LOD component. Regarding the phase-angle estimates shown in Fig. 17 (centre), we can say that these overlap within their uncertainties. According to Fig. 17 (bottom), the variations of the three period time series agree with each other extremely well.

In Fig. 18 (top), the wind plus pressure IB terms χ_3(W) + χ_3(P+IB) of the NMC and JMA systems show similar variations in amplitude like the wind plus pressure terms χ_3(W) + χ_3(P), as seen in Fig. 17 (top). Here, the agreement with the LOD amplitude estimates is just as good. However, their phase estimates displayed in Fig. 18 (centre), especially for the NMC time series until 1988, differ systematically by a few degrees from the LOD estimates. Compared to Fig. 17 (centre), we can see that the phase difference here is even a little larger than there. After that, when the JMA time series

begins, there is good agreement between the estimates of both systems and those of LOD. Concerning the period, it can be seen in Fig. 18 (bottom) that no conformity of the variation exists as obtained for the wind plus pressure terms χ_3(W) + χ_3(P) shown in Fig. 17 (bottom).

It is worth mentioning that the parameter estimates of the wind plus pressure terms χ_3(W) + χ_3(P) of the NMC and JMA systems agree still better with previous estimates obtained for the annual LOD(SLR) component for the years 1986 to 1991 by Höpfner (1996) (see Fig. 1) than with the estimates of the LOD(IERS) component over this time span. Obviously, the reason for this is that the LOD data of the EOP(IERS)C04 series is a combination of individual series that is slightly smoothed; see Section 3.1.

(b) Semiannual oscillation
Given the variation in amplitude of the LOD component and of the wind terms χ_3(W) of the NMC and JMA systems in Fig. 19 (top), it is clearly visible that of the LOD component runs nearly parallel to that of the wind term χ_3(W) of the NMC system. Here, the LOD amplitude is consistently larger by 0.08 ms. The wind term χ_3(W)JMA is characterized by slightly larger amplitude than of the wind term χ_3(W)NMC. In Fig. 19 (centre), note the rather similar variations in phase. However, there are three small disagreements, namely at the beginning and in 1983 of the NMC phase time series and at the end of the phase time series of both systems. As Fig. 19 (bottom) shows, the variations in period with time are quite similar, expect at the beginning of the period time series of the wind term χ_3(W) in the NMC system where a disagreement exists with that of the LOD component. Evidently, the semiannual period estimates of the three components vary between 176 and 189 days. This result coincides with that reported by Höpfner (1996).

Figure 20 shows the same as Fig. 19, but for the wind plus pressure terms χ_3(W) + χ_3(P) instead of the wind terms χ_3(W). A comparison of both figures shows that the agreement between the variations in amplitude is similarly well displayed in Fig. 20 (top) but better in phase and period displayed in Fig. 20 (centre) and Fig. 20 (bottom), respectively. All the limited-period disagreements mentioned above have become smaller.

Figure 21, finally, presents the same as Figs 19 and 20, but for the wind plus pressure IB terms χ_3(W) + χ_3(P+IB). Comparing the Figs 20 and 21, we see similar characteristics of the variations in amplitude, phase and period of the semiannual $\mathrm{LOD}_{\mathrm{atm}}$ components in both systems.

In contrast to the annual oscillation, the previous estimates obtained for the semiannual LOD(SLR) component over 1985 to 1992 by Höpfner (1996) (see Fig. 2) are virtually identical with those of the LOD(IERS) component over this time span.

Concerning the parameter variations of the seasonal $\mathrm{LOD}_{\mathrm{atm}}$ oscillations in the NMC system, it should be pointed out that, as described in Section 3.2, prior to January 1981, the AAM(NMC) data cover the altitude only up to the 100-hPa level and after that up to 50-hPa level. This may be designated in the manner that each $\mathrm{LOD}_{\mathrm{atm}}$ time series is first in the old system and then in new system. Using the designed band-pass filters to separate the annual and semiannual oscillations from the $\mathrm{LOD}_{\mathrm{atm}}$(NMC) time series, we obtain the resulting time series in the old, old-new-mixed and new systems for the following time spans:

Annual oscillation
- in old system till October 29, 1978, i. e. 43810.0 in MJD,
- in old-new-mixed system from October 30, 1978 to March 6, 1983, i. e. from 43811.0 to 45399.0 in MJD and
- in new system from March 7, 1983, i. e. 45400.0 in MJD.

Semiannual oscillation
- in old system till December 4, 1979, i. e. 44211.0 in MJD,
- in old-new-mixed system from December 5, 1979 to January 29, 1982, i. e. from 44212.0 to 44998.0 in MJD and
- in new system from January 30, 1982, i. e. 44999.0 in MJD.

This should be compared with the periods in (b) of Section 5. Regarding this fact, we notice a systematic impact on the amplitude of the annual oscillation of the χ_3(W), χ_3(W) + χ_3(P) and χ_3(W) +χ_3(P+IB) terms; see Figs 16 (top), 17 (top) and 18 (top). Also, the semiannual oscillation is obviously concerned but to a minor extent; see Figs 19 (top), 20 (top) and 21 (top).

It is worth remarking that the annual and semiannual $\mathrm{LOD}_{\mathrm{atm}}$ oscillations are distinguished by the fact that the annual oscillation has an excess amplitude whereas the semiannual oscillation has a shortage amplitude compared to the seasonal LOD oscillations. Ultimately, it is still necessary to judge whether the wind plus pressure term χ_3(W) + χ_3(P) or the wind plus pressure IB term χ_3(W) + χ_3(P+IB) is the better $\mathrm{LOD}_{\mathrm{atm}}$ component. We have found that the annual oscillation of the wind plus pressure term χ_3(W) + χ_3(P) agrees better with that of the LOD component. By contrast, the semiannual oscillation of the wind plus pressure term χ_3(W) + χ_3(P) and that of the wind plus pressure IB term χ_3(W) + χ_3(P+IB) coincide to a larger degree.

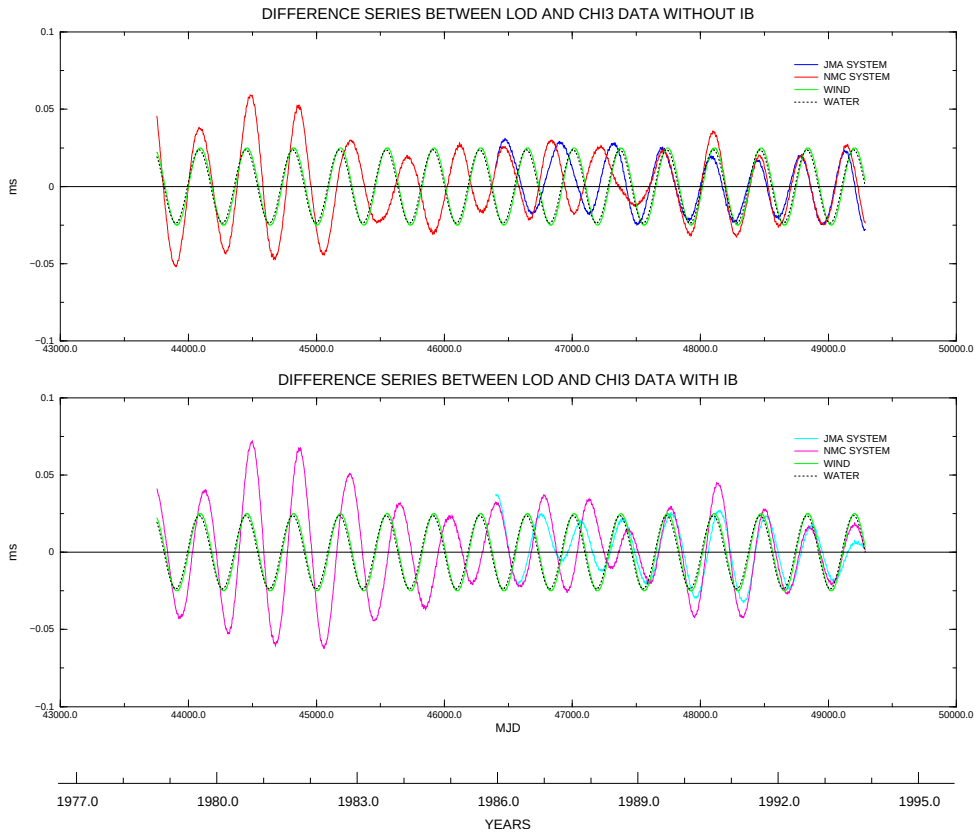

Figure 22. Annual oscillation of the difference series between LOD and $\mathrm{LOD}_{\mathrm{atm}}$ data in the NMC and JMA systems. Top: The $\mathrm{LOD}_{\mathrm{atm}}$ data are those of the χ_3(W) + χ_3(P) terms. Bottom: The $\mathrm{LOD}_{\mathrm{atm}}$ data are those of the χ_3(W) + χ_3(P+IB) terms. Note the wind oscillation of the 10-1 hPa atmospheric layer and the surface-water-induced oscillation estimated by Chao & O'Connor (1988) indicated as curves

7 Seasonal discrepancies in the Earth-atmosphere angular momentum budget

The seasonal imbalances in the solid Earth-atmosphere angular momentum budget must be some combination of measurement error, systematic error, and unmodelled angular momentum exchange. To judge the remaining discrepancies, we have computed the annual and semiannual oscillations in the difference series between the LOD and $\mathrm{LOD}_{\mathrm{atm}}$ data in the NMC and JMA systems, using both the wind plus pressure term χ_3(W) + χ_3(P) and the wind plus pressure IB term χ_3(W) + χ_3(P+IB) as $\mathrm{LOD}_{\mathrm{atm}}$ component. Figures 22 and 23 show the so-called residual oscillations at the annual and semiannual periods, respectively. For the sake of clarity and for later discussion, the data are plotted on larger scales compared to the previous figures. In addition, the ranges of the variations of the oscillation parameters and associated standard deviations are summarized in Table 8. As in Section 6, a comparison of the results referred to the two independent systems NMC and JMA reveals the role of systematic errors in the $\mathrm{LOD}_{\mathrm{atm}}$ data. Discrepancies that are not explainable by measurement and systematic errors suggest significant imbalances in the solid Earth-atmosphere angular momentum budget caused by other excitation sources.

Imbalances may be largely eliminated by incorporating wind data through as much of the height of the atmosphere, including the stratosphere, as possible. Regarding the JMA system, the winds in the atmospheric layer from 10 to 1 hPa are only missing from the solid Earth-atmosphere angular momentum budget. However, according to Rosen and Salstein (1991), they make an important contribution to the momentum budget at the seasonal periods, although the layer represents less than 1% of the atmosphere's mass. The results for the annual and semiannual components of the relative angular momentum of the atmosphere between 1000 and 10 hPa and 1000 and 1 hPa in the NMC and EC systems by Rosen and Salstein (1991) are used to estimate the amplitude and phase of the signals in the 10-1 hPa layer. The estimates obtained are given in Table 9. Here, the phase angle refers to January 1 with respect to the cosine convention. Note that the sign of the amplitude indicates whether the contribution is of positive or negative effect. Accordingly, at the annual period, the wind term neglected from the 10-1 hPa layer is such as to counterbalance the excess of the $\mathrm{LOD}_{\mathrm{atm}}$ oscillation in the JMA system. At the semiannual period, when the term is included in the momentum budget, the discrepancy between LOD and $\mathrm{LOD}_{\mathrm{atm}}$ largely decreases. In Figs 22 and 23, respectively, the annual and semiannual wind oscillations of the 10-1 hPa atmospheric layer denoted by χ_3(W)(10-1) are plotted too.

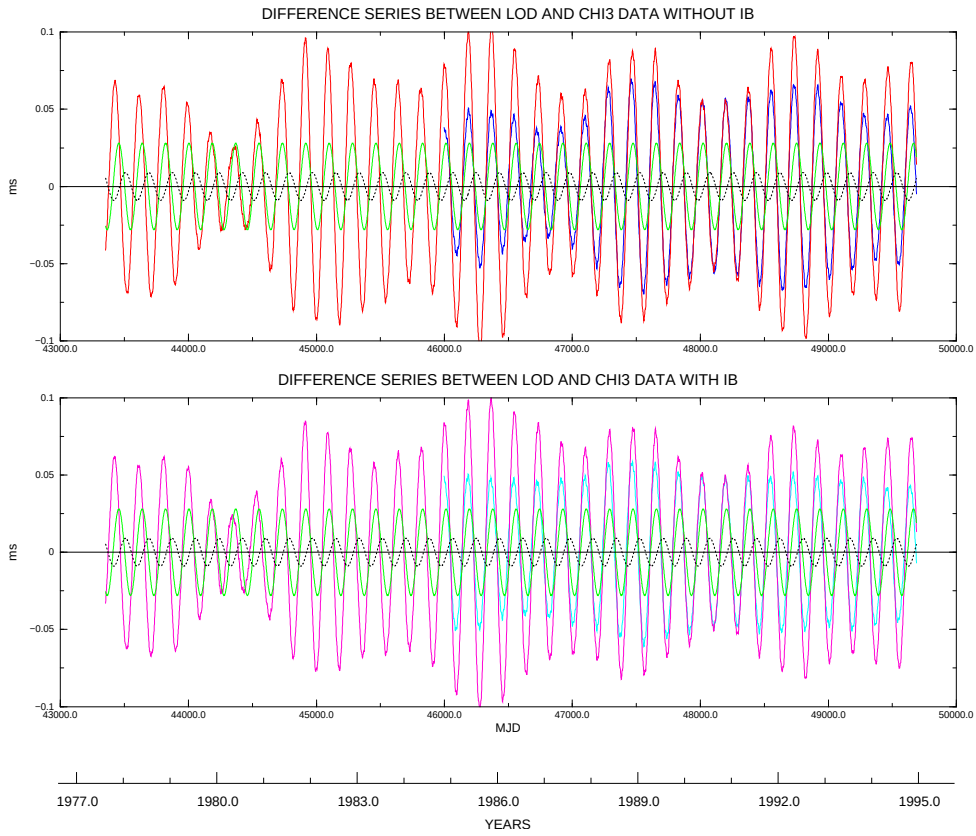

Figure 23. Same as Fig. 22, but for the semiannual oscillation of the difference series between LOD and $\mathrm{LOD}_{\mathrm{atm}}$ data

In Section 2, the surface water-induced variation computed by Chao and O'Connor (1988) has been mentioned, as it may prove to be a significant contribution to the total seasonal, non-tidal oscillations in LOD. Here, these global effects are due to the seasonal mass redistribution of continental surface water storage. Regarding the calculations, it should be noted that these are based on the basic continental water budget equation

$$\Delta h \;=\; p \,-\, e \,-\, r \;, \tag{4}$$

where Δh is the change in surface water storage, p the precipitation including rain and snow, e the evapotranspiration, and r the runoff.

In contrast to the previous studies on the annual wobble excitation caused by surface water variations (see, e. g., van Hylckama 1970; Hinnov and Wilson 1987), the problem by Chao and O'Connor (1988) is considered, which allows for the snow-load contribution from satellite data. The hydrological data used have two parts:

(1) The snow mass distribution according to satellite remote sensing data for 1979-1985; see Chao et al. (1987).
(2) The rain precipitation data according to Willmott, Rowe and Mintz (1985), which are long-term averages for each of the 12 months. Some 50 years of global data went into this averaging process, but the geographical coverage is far from uniform.

The study has excluded Greenland and Antarctica since their mass balance involves snow accumulation, melting, and sublimation on top of moving glacial ice sheets that are largely unknown. According to Chao (personal communication, 1997), the results have not been updated since then. There have been other (presumably more sophisticated) models for the rain precipitation, evapotransportation, and runoff, but the satellite remote sensing still provides the most reliable estimate for snow. Also shown in Figs 22 and 23 are the seasonal contributions from surface water storage estimates on continents by Chao and O'Connor (1988) for more detailed comparisons with the remaining seasonal discrepancies in the solid Earth-atmosphere angular momentum budget.

Furthermore, in Section 2, we have reported on the contribution from the Antarctic Circum-Polar Current estimated by Naito and Kikuchi (1990). Note that this effect is ignored since the portions are an order of the magnitude equal or smaller than the standard deviations of the amplitudes of the residual oscillations at the annual and the semiannual

Table 8. Ranges of the variations of the amplitude, phase and period estimates of the seasonal oscillations of the difference series between LOD and LOD_{atm} data and standard deviations. Min, minimum; Max, maximum; Dif, difference between maximum and minimum; s_0, standard error of a single estimate; $s_{amplitude}$, standard error of an amplitude mean; s_{phase}, standard error of a phase mean; s_{period}, standard error of a period three-point mean; n, number of the pairs; in case of the period, number of the differences

Component from IERS and ...	Period for NMC Min	Max	Dif	Period for JMA Min	Max	Dif	Standard deviations s_0	s_{mean}	n
(a) Annual oscillation									
Amplitude estimates (in ms); $s_{mean} = s_{amplitude}$									
NMC data without IB	0.017	0.057	0.040	0.020	0.042	0.022	±0.006	±0.004	15
with IB	0.009	0.072	0.063	0.009	0.048	0.039	0.008	0.006	15
JMA data without IB				0.019	0.032	0.013	0.005	0.003	8
with IB				0.009	0.039	0.030	0.007	0.005	8
Phase estimates (in degrees); $s_{mean} = s_{phase}$									
NMC data without IB	42.1	292.8	250.7	42.1	212.5	170.4	±29.2	±20.7	13
with IB	220.1	335.7	115.6	220.1	335.7	115.6	23.1	16.3	15
JMA data without IB				56.9	212.6	155.7	26.9	19.0	7
with IB				225.7	324.1	98.4	23.8	16.8	8
Period estimates (in days); $s_{mean} = s_{period}$									
NMC data without IB	313.6	489.3	175.7	313.6	489.3	175.7	±30.7	±17.7	27
with IB	291.5	402.5	111.0	291.5	383.2	91.8	14.7	8.5	29
JMA data without IB				324.6	437.1	112.5	18.1	10.5	12
with IB				283.8	384.4	100.6	17.0	9.8	15
(b) Semiannual oscillation									
Amplitude estimates (in ms); $s_{mean} = s_{amplitude}$									
NMC data without IB	0.026	0.108	0.082	0.055	0.108	0.053	±0.006	±0.004	34
with IB	0.024	0.102	0.078	0.050	0.102	0.052	0.005	0.003	34
JMA data without IB				0.034	0.071	0.037	0.003	0.002	20
with IB				0.041	0.061	0.020	0.003	0.002	20
Phase estimates (in degrees); $s_{mean} = s_{phase}$									
NMC data without IB	195.51	252.69	57.18	219.17	252.69	33.52	±8.41	±5.95	34
with IB	187.06	252.95	65.89	217.06	252.95	35.89	7.89	5.58	34
JMA data without IB				214.78	249.84	35.06	8.02	5.67	20
with IB				203.05	249.98	46.94	9.46	6.69	20
Period estimates (in days); $s_{mean} = s_{period}$									
NMC data without IB	172.90	192.48	19.59	172.90	189.18	16.28	±4.15	±2.40	67
with IB	165.86	198.02	32.16	174.28	188.62	14.34	3.78	2.18	67
JMA data without IB				171.54	190.60	19.07	3.63	2.10	38
with IB				170.01	189.63	19.62	3.68	2.12	38

periods; compare the amplitude estimates of the seasonal Antarctic Circum-Polar Current terms from Table 2 with the corresponding uncertainties given in Table 8.

First, it is not surprising to discover that the results displayed in Figs 22 and 23 and Table 8 confirm the earlier judgment of the seasonal oscillations of the LOD_{atm} time series in the NMC and JMA systems; see Section 6. We shall discuss separately the annual and semiannual residual oscillations:

(a) Annual residual oscillation

Figure 22 (top) shows the annual residual oscillations derived as difference series between LOD and LOD_{atm} data without IB effect in the NMC and JMA systems and Fig. 22 (bottom) the same but with IB effect. Concerning the results

Table 9. Contribution of the wind term neglected from the 10-1 hPa layer to seasonal oscillations in LOD

Term	Period	Annual oscillation Amplitude (in ms)	Phase (in degrees)	Semiannual oscillation Amplitude (in ms)	Phase (in degrees)
Wind (NMC)(10-1)	1980 ... 1985	-0.025	35.0	+0.028	256.3
(EC)(10-1)		-0.025	33.5	+0.028	254.3

in NMC system, notice the residual components between the LOD data and $\mathrm{LOD}_{\mathrm{atm}}$ data in terms of the χ_3(W) + χ_3(P) and χ_3(W) + χ_3(P+IB), respectively, with a clearly larger amplitude during the time span for the old-new-mixed system due to the change of the top level from 100 up to 50 hPa in computing the χ_3(W) values since January 1981; see Sections 2 and 6 for details. For the JMA period, there is generally good agreement between the curves of the NMC and JMA systems. Here, those inferred by the wind plus pressure term χ_3(W) + χ_3(P) agree better than those inferred by the wind plus pressure IB term χ_3(W) + χ_3(P+IB), i. e. the inverted barometer effect makes each residual oscillation somewhat larger in its amplitude and worse in its similarity to that in the other system. In other words, the results inferred without IB effect represent the better estimates.

At the annual period, the residual components in the NMC and JMA systems for the JMA time span have a similar amplitude of about 0.025 ms. Regarding their changes with time, we see good agreement, in particular from 1989 to the end of the series. Since the χ_3(W) data of JMA cover the altitude up to the 10-hPa level, whereas those of NMC integrate winds only up to the 50-hPa level, as reported in Section 2, we regard the JMA results as more significant than those of NMC. This assessment coincides with the range of the amplitude variations and the appropriate standard deviations given in Table 8.

A comparison of the JMA curve with that of the wind signal in the 10-1 hPa atmospheric layer in Fig. 22 (top) shows that there is very good agreement in amplitude. Note also their quite similar variations for a definite period. Considering that the amplitude and phase estimates of the annual contribution represent average values referred to a relatively short time span, the annual significant residual oscillation could be explained by this effect, where the excess amplitude of the annual $\mathrm{LOD}_{\mathrm{atm}}$ component in terms of χ_3(W) + χ_3(P) JMA to LOD is perfectly counterbalanced for most of the time; cf. Fig. 17 (top). At the annual period, thus, the wind term of χ_3(W)(10-1) is apparently responsible for the continuing significant imbalance in the solid Earth-atmosphere angular momentum budget in the JMA system at the achieved level of uncertainty.

The surface-water-induced oscillation is nearly identical with the wind signal in the 10-1 hPa atmospheric layer, as Fig. 22 (top) exhibits as well. Therefore, the same remarks as given about the wind contribution can be made about the hydrological contribution. Since the annual term of χ_3(W)(10-1), if added to that of $\mathrm{LOD}_{\mathrm{atm}}$, could bring the LOD and $\mathrm{LOD}_{\mathrm{atm}}$ oscillations into very close agreement, the estimate from surface water storage (as computed by Chao and O'Connor 1988) appears to be too large. Undoubtedly, this process does contribute to the annual oscillation in LOD, but at some level of precision, as Rosen and Salstein (1991) assert.

(b) Semiannual residual oscillation

Similar to Fig. 22, the semiannual residual oscillations derived as difference series between LOD and $\mathrm{LOD}_{\mathrm{atm}}$ data without IB effect in the NMC and JMA systems are illustrated in Fig. 23 (top) and the same but with IB effect in Fig. 23 (bottom). Note that the residuals inferred both without and with IB effect in NMC system show amplitudes varying with time considerably. In comparison with those in JMA system, they are generally larger. As for the annual frequency, larger systematic errors in the $\mathrm{LOD}_{\mathrm{atm}}$ data of NMC versus JMA provide the more likely explanation for the disagreement. Essentially, the discrepancies remain because of the exclusion of the part of the stratosphere above the 100-hPa and 50-hPa levels, respectively; see again Sections 2 and 6 for details. However, the results inferred from the wind plus pressure term χ_3(W) + χ_3(P) in both systems differ more than those inferred from the wind plus pressure IB term χ_3(W) + χ_3(P+IB) in difference to the annual oscillation, i. e. the inverted barometer effect makes each residual oscillation mostly somewhat smaller in its amplitude and better in its similarity to that in the other system. In other words, the results inferred with IB effect represent the better estimates.

At the semiannual period, we regard the JMA results as more significant than those of NMC, as for the annual period. This assessment is based on the amplitude estimates varying only between 0.041 and 0.061 ms in JMA system, while those of NMC show a variation ranging from 0.050 to 0.102 ms for the same period; for details see the results and standard deviations of the semiannual residual oscillation summarized in Table 8.

A comparison of the JMA curve with that of the wind signal in the 10-1 hPa atmospheric layer in Fig. 23 (bottom) shows that the semiannual residual oscillation could be due to the neglect of the semiannual χ_3(W)(10-1) term to a high degree. Then, the remainder is explained by the surface water storage that may be contributed in the magnitude as the amplitude estimated by Chao and O'Connor (1988). Here, the contribution to the semiannual $\mathrm{LOD}_{\mathrm{atm}}$ component in terms of χ_3(W) + χ_3(P+IB)JMA must be positive; cf. Fig. 21 (top). Thus, the Earth's axial angular momentum budget for the semiannual oscillation in JMA system is most likely closed with the wind contribution of the upper stratosphere and the hydrological contribution considering the uncertainties.

Finally, note that the annual residual oscillation is comparatively more changeable in phase and period than the semi-annual residual oscillation; compare Fig. 22 with Fig. 23. Regarding the understanding of the Earth's axial momentum balance at annual and semiannual periods, our findings concerning the pressure terms coincide with those based on LOD(IRIS) and $\mathrm{LOD}_{\mathrm{atm}}$(JMA) data from 1984 to 1988 by Naito and Kikuchi (1990); see Section 2 and for more details the original article. As shown above, the pressure terms without IB effect χ_3(P) and with IB effect χ_3(P+IB), respectively,

are contributing to the annual and semiannual oscillations in LOD, although their data are doing so at levels smaller the error in those of the wind term χ_3(W); cf. Rosen and Salstein (1991). With respect to balancing the seasonal global momentum budget, we support the assertion by Rosen and Salstein (1991) that the residual imbalances may be explained by incorporating the momentum of the entire stratosphere. Only after this has been done, one may look for a different excitation source, such as changes in the global surface water redistribution.

8 Retrospect and concluding remarks

The significant improvements in geodetic and atmospheric data sets during the last decade have enabled studies of the solid Earth-atmosphere momentum budget with increasingly finer temporal resolution. Even so, at seasonal periods, there is continuing interest in understanding variations in the Earth's axial angular momentum budget. For this, there are several reasons. As mentioned in the Introduction, the seasonal cycle in LOD represents the largest signal on less than decadal time scales. Therefore, the studies started with respect to the seasonal LOD oscillations. Then, the subject was extended to the global axial angular momentum budget. Since various processes may make seasonal contributions to the budget, the studies were multidisciplinary. Especially for the hydrosphere as another essential excitation source, there are still no remarkable advances. Up to now, concerning the oceanic contribution, the idealized extreme of completely isostatic response of the oceans to pressure changes in terms of the inverted barometer model is assumed. By using the continental water budget equation, the contribution of the surface water storage on continents was estimated in an averaging process.

The objective of this study has been to quantify better the seasonal imbalances in the solid Earth-atmosphere axial angular momentum budget. For this purpose, the data of the following time series at one-day intervals have been used:

(a) LOD of EOP(IERS)C04 from 1962 to 1995,
(b) $\mathrm{LOD}_{\mathrm{atm}}$ in terms of χ_3(W), χ_3(P) and χ_3(P+IB) of AAM(NMC) from 1976 to 1995 and
(c) $\mathrm{LOD}_{\mathrm{atm}}$ in terms of χ_3(W), χ_3(P) and χ_3(P+IB) of AAM(JMA) from 1983 to 1995.

By comparison of the LOD and $\mathrm{LOD}_{\mathrm{atm}}$ diagrams, the data sets clearly prove that the Earth and its atmosphere are closely coupled dynamically. For more detailed comparisons of the relationship between the time series, we have computed their correlations. As expected, the results confirm that the relationship of LOD is somewhat higher to the wind term χ_3(W) combined with the pressure terms χ_3(P) and χ_3(P+IB), respectively, than to the wind term χ_3(W) alone. Another result is that the seasonal oscillations of LOD should be corrected for the tidal effects Sa and Ssa for comparisons with those of $\mathrm{LOD}_{\mathrm{atm}}$.

The analysis procedures consist of two steps: (a) Filtering out the annual and semiannual oscillations from the original data sets and (b) calculating optimal estimates of the amplitude, phase and period of each oscillation.

For separating the main components (including the trend), we have applied zero-phase digital filters, which quantify the small signals of the pressure terms χ_3(P) and χ_3(P+IB) quite well. Then, for computing the parameter estimates, we used a simple method based on the maximum, zero passage and minimum of a periodic function.

At the annual and semiannual periods, all the oscillations filtered out from the LOD and $\mathrm{LOD}_{\mathrm{atm}}$ time series vary in amplitude, phase and period with time at a statistically significant level. The role of systematic errors in them has been discussed from a comparison of the analyses of the LOD(IERS), $\mathrm{LOD}_{\mathrm{atm}}$(NMC) and $\mathrm{LOD}_{\mathrm{atm}}$(JMA) data. Also included are the previous results derived from the LOD(SLR) data computed by the GFZ in terms of series ERP(GFZ)L04 1983-1993, where there exists a good agreement between the seasonal LOD(IERS) and LOD(SLR) oscillations.

Especially at the annual period, the results of LOD agree better with those of $\mathrm{LOD}_{\mathrm{atm}}$(JMA) than with those of $\mathrm{LOD}_{\mathrm{atm}}$(NMC). This outcome was expected, since the wind term χ_3(W) of the AAM(NMC) series does not incorporate much of the stratosphere, having its upper boundaries limited to either 100 or 50 hPa, whereas that of the AAM(JMA) series includes the level up to 10 hPa. Compared to the annual oscillations of $\mathrm{LOD}_{\mathrm{atm}}$, that of LOD has the smaller amplitude. Here, the amplitude variations with time are rather similar. By incorporating the wind term χ_3(W) with the pressure terms χ_3(P) and χ_3(P+IB), respectively, there are much minor amplitude differences between the $\mathrm{LOD}_{\mathrm{atm}}$ and LOD components. Considering the phase and period variations, the annual oscillation of the wind plus pressure term χ_3(W) + χ_3(P) is to judge as the better $\mathrm{LOD}_{\mathrm{atm}}$ component.

Like to the annual oscillation, the semiannual results of LOD show better agreement with those of $\mathrm{LOD}_{\mathrm{atm}}$(JMA) than those of $\mathrm{LOD}_{\mathrm{atm}}$(NMC). This is for the same reason given above for the annual period. On the contrary, the amplitude of the semiannual LOD oscillation is consistently larger than those of $\mathrm{LOD}_{\mathrm{atm}}$ in both systems. Concerning the temporal variations in amplitude of the components, notice good parallelism of the curves. For the phase and period variations, see similar characteristics. Unlike to the annual oscillation, the semiannual oscillations of the $\mathrm{LOD}_{\mathrm{atm}}$ components in terms of χ_3(W) + χ_3(P) and χ_3(W) + χ_3(P+IB) do not differ clearly.

To judge the seasonal discrepancies in the solid Earth-atmosphere angular momentum budget, we have used the residual oscillations as computed from the difference series between the LOD and $\mathrm{LOD}_{\mathrm{atm}}$ data in the NMC and JMA systems at the annual and semiannual periods. If winds through the entire troposphere and stratosphere are included in the momentum budget, then imbalances may largely be eliminated. In case of the JMA system, the signals in the 10-1 hPa atmospheric layer only are missing. Therefore, we have decided that the JMA results are more significant than those of NMC. Regarding the IB effect, we found that the residual values inferred without IB effect represent the better estimates at the annual period but those inferred with IB effect represent the better ones at the semiannual period.

As the seasonal residual oscillations in JMA system exhibit, there are significant imbalances, where the amplitude average is about 0.025 ms at the annual period and about 0.055 ms at the semiannual period; see Figs 22 and 23. The wind terms at levels from 1000 to 10 hPa and from 1000 to 1 hPa in the NMC and EC systems estimated by Rosen and Salstein (1991) are used in computing the impact of winds in the 10-1 hPa layer. In addition, the surface-water-induced oscillations computed by Chao anand O'Connor (1988) served for comparisons with the residual components. At the annual period, the significant imbalance could be explained by the missing wind term in the 10-1 hPa layer counterbalancing the excess of the $\mathrm{LOD}_{\mathrm{atm}}$(JMA) oscillation. According to this, the changes in the distribution of surface water storage should only contribute at higher levels of precision, i. e. that the estimate used as a comparison value is revealed to be immoderately. At the semiannual period, the wind term in the 10-1 hPa layer does not achieve a balance in the budget, and a hydrological contribution, as estimated quantitatively, should nearly close the global momentum budget.

Our analysis has established that there seems little need to invoke processes other than atmospheric ones before the precision of the atmospheric angular momentum data has been improved. Connected with this, it is necessary to extend the upper limit into the upper stratosphere up to the 1-hPa level in computing the wind term χ_3(W). In addition, the determination of the oceanic contribution to pressure term χ_3(P) will require a model of the dynamic response of the oceans to pressure changes more sophisticated than the inverted barometer model included in the pressure term χ_3(P+IB). Also, the role of the mountain and surface friction torques deserves special attention. If the data sets of LOD and $\mathrm{LOD}_{\mathrm{atm}}$ are accurate enough, then their analysis will prove reliably whether the seasonal momentum budget is closed or whether a significant excitation source has been omitted. Undoubtedly, non-wind processes, especially the hydrological ones, play a role in the global momentum budget at high level of precision. Therefore, the effects of such phenomena have to be dealt with in the future.

References

Barnes, R. T. H., Hide, R., White, A. A. and Wilson, C. A., 1983. Atmospheric angular momentum fluctuations, length-of-day changes and polar motion. *Proc. Roy. Soc. Lond. A, 387*, 31–73.

Chao, B. F. and O'Connor, W. P., 1988. Global surface-water-induced seasonal variations on the Earth's rotation and gravitational field. *Geophys. J., 94*, 263–270.

Chao, B. F., O'Connor, W. P., Chang, A. T. C., Hall, D. K. and Foster, J. L., 1987. Snow-load effect on the Earth's rotation and gravitational field, 1979-1985. *J. Geophys. Res., 92*, 9415–9422.

Dickman, S. R., 1991. Ocean tides for satellite geodesy. *Mar. Geod., 14*, 21–56.

Eubanks, T. M., Steppe, J. A. and Dickey, J. O., 1985a. The atmospheric excitation of Earth orientation changes during MERIT. *Proc. Int. Conf. on the Earth Rotation and Terrestrial Reference Frame. Vol. 2*, 469–483.

Eubanks, T. M., Steppe, J. A., Dickey, J. O. and Callahan, P. S., 1985b. A spectral analysis of the Earth's angular momentum budget. *J. Geophys., 90*, 5385–5404.

Freedman, A. P., Steppe, J. A., Dickey, J. O., Eubanks, T. M. and Sung, L.-Y., 1994. The short-term prediction of universal time and length of day using atmospheric angular momentum. *J. Geophys. Res., 99*, B4, 6981–6996.

Greiner-Mai, H., 1993. Decade variations of the Earth's rotation and geomagnetic core-mantle coupling. *J. Geomag. Geoelectr., 45*, 1333–1345.

Greiner-Mai, H., 1995. About possible geophysical causes of the decade fluctuations in the length of day. *Astron. Nachr., 316*, 5, 311–318.

Großmann, W., 1953. *Grundzüge der Ausgleichungsrechnung*. Springer-Verlag, Berlin / Göttingen / Heidelberg.

Gu, Z. N. and Paquet, P., 1993. A possible contribution of the solar wind to annual fluctuation in the length of day. *Earth, Moon, and Planets, 62*, 3, 259–271.

Hide, R., Birch, N. T., Morrison, L. V., Shea, D. J. and White, A. A., 1980. Atmospheric Angular Momentum Fluctuations and Changes in the Length of Day. *Nature, 286*, 114–117.

Hide, R. and Dickey, J. O., 1991. Earth's Variable Rotation. *Science, 253*, 629–637.

Hinnov, L. A. and Wilson, C. R., 1987. An estimate of the water storage contribution to the excitation of polar motion. *Geophys. J. R. astr. Soc., 88*, 437–459.

Höpfner, J., 1995a. Periodische Anteile in der Erdrotation und dem atmosphärischen Drehimpuls und ihre Genauigkeiten. *ZfV, 120*, 1, 8–16.

Höpfner, J., 1995b. Atmosphärische und nicht-atmosphärische Erregung der saisonalen Erdrotationsschwankungen. *AVN, 102*, 2, 65–74.

Höpfner, J., 1996. Seasonal Oscillations in Length-Of-Day. *Astron. Nachr., 317*, 4, 273–280.

IERS, 1995. *1994 IERS Annual Report*. Central Bureau of IERS. Observatoire de Paris.

Lambeck, K., 1980. *The Earth's Variable Rotation: Geophysical Causes and Consequences*. Cambridge University Press, New York.

McCarthy, D. D. (ed.), 1992. *IERS Conventions (1992)*. IERS Technical Note 13, Central Bureau of IERS. Observatoire de Paris.

Munk, W. H. and MacDonald, G. J. F., 1960. *The rotation of the Earth*. Cambridge University Press, New York.

Munk, W. H. and Miller, R. L., 1950. Variations in the Earth's Angular Velocity Resulting from Fluctuations in Atmospheric and Oceanic Circulation. *Tellus, 2*, 93–101.

Naito, I. and Kikuchi, N., 1990. A seasonal budget of the Earth's axial angular momentum. *Geophys. Res. Lett., 17*, 5, 631–634.

Naito, I., Kikuchi, N. and Yokoyama, K., 1987. Results of Estimating the Effective Atmospheric Angular Momentum Functions Based on the JMA Global Analysis Data. *Publ. Int. Lat. Obs. Mizusawa, 20*, 1 & 2, 1–11.

Pavel, F. and Uhink, W., 1935. Die Quarzuhren des Geodätischen Instituts in Potsdam. *Astron. Nachr.*, *257*, 356–390.
Rosen, R. D., 1993. The axial momentum balance of Earth and its fluid envelope. *Surveys in Geophysics*, *14*, 1–29.
Rosen, R. D. and Salstein, D. A., 1985. Contribution of Stratospheric Winds to Annual and Semiannual Fluctuations in Atmospheric Angular Momentum and the Length of Day. *J. Geophys. Res.*, *90*, B1, 8033–8041.
Rosen, R. D. and Salstein, D. A., 1991. Comment on ”A seasonal budget of the Earth’s axial angular momentum” by Naito and Kikuchi. *Geophys. Res. Lett.*, *18*, 10, 1925–1926.
Rosen, R. D., Salstein, D. A., Miller, A. J. and Arpe, K., 1987. Accuracy of atmospheric angular momentum estimates from operational analyses. *Mon. Weather Rev.*, *115*, 1627–1639.
Rosen, R. D., Salstein, D. A. and Wood, T. M., 1990. Discrepancies in the Earth-Atmosphere Angular Momentum Budget. *J. Geophys. Res.*, *95*, B1, 265–279.
Salstein, D. A. and Rosen, R. D., 1985. Computations of atmospheric angular momentum, with emphasis on the MERIT period. *Proc. Int. Conf. on the Earth Rotation and Terrestrial Reference Frame. Vol. 2*, 440–449.
Salstein, D. A., Kann, D. M., Miller, A. J. and Rosen, R. D., 1993. The Sub-bureau for Atmospheric Angular Momentum of the International Earth Rotation Service: A Meteorological Data Center with Geodetic Applications. *Bull. Ann. Met. Soc.*, *74*, 1, 67–80.
Stoyko, N., 1936. *Bull. Horaire du Bureau International de I’Heure*. Observatoire de Paris.
Van Hylckama, T. E. A., 1970. Water balance and Earth unbalance. Int. Ass. Sci. Hydrology. *Proc. Read. Symp. World Water Balance*, *92*, 434–444.
Whitworth, T. and Peterson, R. G., 1985. Volume transport of the Antarctic Circum-Polar Current from bottom pressure measurements. *J. Phys. Oceanogr.*, *15*, 810–816.
Willmott, C. J., Rowe, C. M. and Mintz, Y., 1985. Climatology of the terrestrial seasonal water cycle. *J. Climatol.*, *5*, 589–606.
Yoder, C.F., Williams, J. G. and Parker, M. E., 1981. Tidal variations of Earth rotation. *J. Geophys. Res.*, *86*, 881–891.
Zhao, J. and Qu. W., 1995. Study of the dynamical mechanism of seasonal variation of Earth’s rotational velocity. *J. Geophys. Res.*, *100*, B7, 12719–12730.